

# The Deubiquitylase USP2 Regulates the LDLR Pathway by Counteracting the E3-Ubiquitin Ligase IDOL

Jessica Kristine Nelson,\* Vincenzo Sorrentino,\* Rossella Avagliano Trezza, Claire Heride, Sylvie Urbe, Ben Distel, Noam Zelcer

**Rationale:** The low-density lipoprotein (LDL) receptor (LDLR) is a central determinant of circulating LDL-cholesterol and as such subject to tight regulation. Recent studies and genetic evidence implicate the inducible degrader of the LDLR (IDOL) as a regulator of LDLR abundance and of circulating levels of LDL-cholesterol in humans. Acting as an E3-ubiquitin ligase, IDOL promotes ubiquitylation and subsequent lysosomal degradation of the LDLR. Consequently, inhibition of IDOL-mediated degradation of the LDLR represents a potential strategy to increase hepatic LDL-cholesterol clearance.

**Objective:** To establish whether deubiquitylases counteract IDOL-mediated ubiquitylation and degradation of the LDLR.

**Methods and Results:** Using a genetic screening approach, we identify the ubiquitin-specific protease 2 (USP2) as a post-transcriptional regulator of IDOL-mediated LDLR degradation. We demonstrate that both USP2 isoforms, USP2-69 and USP2-45, interact with IDOL and promote its deubiquitylation. IDOL deubiquitylation requires USP2 enzymatic activity and leads to a marked stabilization of IDOL protein. Paradoxically, this also markedly attenuates IDOL-mediated degradation of the LDLR and the ability of IDOL to limit LDL uptake into cells. Conversely, loss of USP2 reduces LDLR protein in an IDOL-dependent manner and limits LDL uptake. We identify a tri-partite complex encompassing IDOL, USP2, and LDLR and demonstrate that in this context USP2 promotes deubiquitylation of the LDLR and prevents its degradation.

**Conclusions:** Our findings identify USP2 as a novel regulator of lipoprotein clearance owing to its ability to control ubiquitylation-dependent degradation of the LDLR by IDOL. (*Circ Res.* 2016;118:410-419. DOI: 10.1161/CIRCRESAHA.115.307298.)

**Key Words:** E3 ubiquitin ligase ■ LDL cholesterol ■ LDL receptors ■ MYLIP/IDOL ■ ubiquitin ■ USP2

The low-density lipoprotein (LDL) receptor (LDLR) is a major determinant of circulating levels of LDL.<sup>1</sup> Accordingly, mutations in this receptor are the leading cause for development of autosomal-dominant hypercholesterolemia, a disease characterized by reduced hepatic LDL clearance, elevated plasma cholesterol levels, and accelerated atherosclerosis.<sup>2,3</sup> Owing to its central role in lipoprotein metabolism, the level of the LDLR is subject to tight homeostatic regulation. Transcription of the *LDLR* is controlled by the sterol regulatory element-binding proteins, and it is increased when cellular cholesterol levels decline to allow increased endocytosis of cholesterol-rich LDL particles.<sup>4,5</sup>

LDLR abundance. Among these, ubiquitylation of the LDLR plays an important role in controlling the intracellular trafficking of the receptor,<sup>6,7</sup> similar to the role this process plays for other membrane receptors. We have recently identified inducible degrader of the LDLR (IDOL) as an E3-ubiquitin ligase (E3) that specifically promotes ubiquitylation of the LDLR.<sup>8</sup> IDOL itself is subject to direct transcriptional regulation by the sterol-sensing transcription factors liver X receptors (LXR). Activation of LXR when cellular sterol levels increase leads to induction of *IDOL* expression and activity, and subsequent ubiquitylation of conserved residues in the short intracellular tail of the LDLR. In turn, ubiquitylation of the LDLR serves to mark the receptor for internalization and subsequent lysosomal degradation.<sup>8</sup> In particular, the plasma membrane pool of LDLR is highly sensitive to IDOL activity, and ubiquitylation leads to rapid removal of this receptor pool via an epsin-dependent but clathrin-independent endocytic

**In This Issue, see p 367  
Editorial, see p 371**

Next to transcriptional regulation, post-transcriptional mechanisms are also emerging as important determinants of

Original received July 28, 2015; revision received December 8, 2015; accepted December 14, 2015. In November 2015, the average time from submission to first decision for all original research papers submitted to *Circulation Research* was 15.52 days.

From the Department of Medical Biochemistry, Academic Medical Center of the University of Amsterdam, Amsterdam, The Netherlands (J.K.N., V.S., R.A.T., B.D., N.Z.); and Department of Cellular and Molecular Physiology, University of Liverpool, Liverpool, United Kingdom (C.H., S.U.).

\*These authors contributed equally to this article.

The online-only Data Supplement is available with this article at <http://circres.ahajournals.org/lookup/suppl/doi:10.1161/CIRCRESAHA.115.307298/-/DC1>.

Correspondence to Noam Zelcer, PhD, Department of Medical Biochemistry, Meibergdreef 15, 1105AZ Amsterdam, The Netherlands. E-mail [n.zelcer@amc.uva.nl](mailto:n.zelcer@amc.uva.nl)  
© 2015 American Heart Association, Inc.

*Circulation Research* is available at <http://circres.ahajournals.org>

DOI: 10.1161/CIRCRESAHA.115.307298

**Nonstandard Abbreviations and Acronyms**

<b>E3</b>	E3-ubiquitin ligase
<b>IDOL</b>	inducible degrader of the LDLR
<b>LDLR</b>	low-density lipoprotein receptor
<b>LXR</b>	liver X receptors
<b>USP</b>	ubiquitin-specific protease

route.<sup>6</sup> The role of IDOL in human lipoprotein metabolism is supported by genome-wide association studies that identify an association between genetic variation in the *IDOL* locus and circulating levels of LDL-cholesterol.<sup>9,10</sup> Furthermore, we recently described a rare loss-of-function *IDOL* variant in individuals with LDL-cholesterol.<sup>11</sup> Consistent with this, silencing of *IDOL* in nonhuman primates using an RNAi-based approach resulted in a reduction of circulating levels of LDL-cholesterol, which was associated with increased levels of hepatic LDLR protein.<sup>12</sup> Thus, the LXR–IDOL–LDLR axis is a potent ubiquitylation-dependent mechanism to acutely limit lipoprotein-derived cholesterol uptake.<sup>13,14</sup>

Similar to other post-translational modifications, ubiquitylation is reversible; a process dependent on the activity of deubiquitylases.<sup>15</sup> The human genome encodes ≈100 deubiquitylases, 79 of which are predicted to be active.<sup>16,17</sup> These deubiquitylases are classified into 5 distinct families, the largest being the ubiquitin-specific protease (USP) family. A major challenge in elucidating the cellular function and physiological roles of deubiquitylases is identification of their substrate specificity.<sup>16,18</sup> Adding to the complexity, recent studies indicate that in addition to removing or remodeling ubiquitin (chains) from ubiquitylated substrates, deubiquitylases may also act directly on E3s, thereby modifying the stability and activity of the latter.<sup>19,20</sup> Characterizing the deubiquitylase–E3 interactome thus represents an important step in understanding how E3s are themselves regulated by ubiquitylation.<sup>17,21</sup>

Whether deubiquitylases play a role in cholesterol metabolism is largely unknown. Our work and that of Scotti et al<sup>7</sup> have recently shown that activity of the endosomal-sorting complex required for transport–associated USP8 is required for IDOL-dependent degradation of ubiquitylated LDLR.<sup>6</sup> However, this most likely represents a nonselective deubiquitylation step used to salvage ubiquitin from ubiquitylated cargo before it entering multivesicular bodies. Given its potent LDLR-lowering activity, we hypothesized that the IDOL pathway may be itself subject to post-transcriptional regulation, in addition to transcriptional control by LXRs. Herein, we identify USP2 as a negative regulator of IDOL-dependent degradation of the LDLR, thereby implicating this deubiquitylase as a regulator of lipoprotein metabolism.

**Methods**

A brief description of the methods is provided below. Detailed description of the methods are available at the Online Data Supplement.

**Cell Culture and Transfections**

HEK293T, HeLa, Huh7, and HepG2 cells were obtained from the ATCC and maintained in DMEM supplemented with 10% fetal bovine serum at 37°C and 5% CO<sub>2</sub>. A431 cells were a kind gift from Drs Vilja Pietiainen and Elina Ikonen (University of Helsinki). Wild-type

and *Idol*<sup>−/−</sup> mouse embryonic fibroblasts (MEFs) were a kind gifts from Dr Peter Tontonoz (University of California at Los Angeles). DU145 were from Dr Koen van de Wetering (NKI, Amsterdam). Where indicated, cells were sterol depleted by culture in sterol-depletion medium (DMEM supplemented by 10% lipoprotein-deficient serum, 5 μg/mL simvastatin, and 100 μmol/L mevalonate) or treated with 1 μmol/L GW3965 to induce LXR signaling. HEK293T and HepG2 cells were transfected with the indicated amounts of plasmids using the JetPrime reagent, and transfection efficiency was monitored by cotransfection of a GFP expression plasmid.

**Plasmids and Expression Constructs**

Expression plasmids encoding IDOL, LDLR, USP8, very low-density lipoprotein receptor, GFP, Ubiquitin, and Epsin1 were previously reported.<sup>6,8,22</sup> Expression plasmids encoding *USP2-69* and *USP2-45* cDNAs were generated with gateway-mediated recombination (Invitrogen). Unless otherwise indicated, *USP2-69* is referred to as USP2. The activity disabling C276A<sup>23,24</sup> mutation in USP2 was introduced using the QuikChange site-directed mutagenesis kit. All plasmids used in this study experiments were isolated by CsCl<sub>2</sub> gradient centrifugation and their correctness verified by sequencing.

**Antibodies and Immunoblot Analysis**

Total cell lysates were prepared in radioimmunoprecipitation assay buffer (RIPA; 150 mmol/L NaCl, 1% Nonidet P-40, 0.1% sodium deoxycholate, 0.1% SDS, 100 mmol/L Tris-HCl, and pH 7.4) supplemented with protease inhibitors. Lysates were cleared by centrifugation at 4°C for 10 minutes at 10000 g. Samples were separated on NuPAGE BisTris gels and transferred to nitrocellulose. The primary antibodies used are listed in the extended Methods section in Online Data Supplement. Secondary HRP (horseradish peroxidase)-conjugated antibodies were used and visualized with enhanced chemiluminescence. All immunoblots are representative of at least 3 independent experiments.

**LDL Uptake Assay**

DyLight 488-labeled LDL was produced as previously described.<sup>25</sup> Briefly, HepG2, HeLa, or A431 cells were incubated in sterol-depletion medium for 16 hours before addition of LDL to increase LDLR abundance. To initiate LDL uptake, cells were incubated with 5 μg/mL DyLight488-labeled LDL in DMEM supplemented with 0.5% BSA at 37°C. Subsequently, cells were washed twice with PBS supplemented with excess sterols (PBS with 10% FCS), followed by an additional wash with PBS. Endocytosis of LDL was determined by lysing cells in RIPA buffer and quantification of the fluorescence signal on a Typhoon imager. Relative LDL uptake was calculated from the measure of fluorescence values corrected for specific uptake (cells treated with labeled LDL in the presence of an excess of nonlabeled LDL) and presented as mean±SD.

**Measurement of Cell Surface LDLR**

Surface LDLR density in the different cells was determined as previously reported.<sup>6</sup> Briefly, cells were treated as indicated, dissociated, and incubated in fluorescence-activated cell sorter blocking buffer for 30 minutes on ice. Subsequently, 100000 cells were stained with a R-Phycoerythrin-conjugated mouse antihuman LDLR antibody for 1 hour on ice. Cells were subsequently washed 3× with fluorescence-activated cell sorter buffer and directly analyzed on a fluorescence-activated cell sorter Calibur Flow Cytometer (BD Biosciences). Relative surface LDLR was calculated from geomean values after correction for background using FlowJo, and presented as mean±SD.

**siRNA Transfection**

To knockdown *USP2* expression, we used ON-TARGETplus Human USP2 SMARTpool (Dharmacon: cat#L-006069-00), or individual ON-TARGETplus Human USP2 siRNAs (Dharmacon: cat#J-006069-11-13). As control, we used the ON-TARGETplus Non-targeting Pool (Dharmacon: cat#D001810-10). A431 and HeLa cells were transfected with siRNAs (30 nmol/L) using the JetPrime reagent. HepG2 and DU145 cells were transfected similarly, but with the RNAiMAX reagent. The efficiency of *USP2* silencing was assessed by quantitative polymerase chain reaction. Unless otherwise indicated, siRNA transfection experiments were conducted for 48 hours.

## RNA Isolation and Quantitative Polymerase Chain Reaction

Total RNA was isolated from cells using TRIzol and 1  $\mu$ g of total RNA was reverse transcribed using the iScript reverse transcription reagent. SYBR Green real-time quantitative polymerase chain reaction assays were performed on a Lightcycler 480 II apparatus. Oligonucleotide sequences are available on request.

## Yeast-2-Hybrid Screen

*Saccharomyces cerevisiae* strains used in this study are PJ69-4a (*trp1-901 leu2-3,112 ura3-52 his3-200 gal4D gal80D LYS2::GAL1-HIS3 GAL2-ADE2 met2::GAL7-lacZ*) and PJ69-4 $\alpha$  (*trp1-901 leu2-3,112 ura3-52 his3-200 gal4D gal80D LYS2::GAL1-HIS3 GAL2-ADE2 met2::GAL7-lacZ*). Cells were grown at 28°C in YPAD or in minimal glucose medium. PJ69-4 $\alpha$  transformed with human IDOL constructs or LDLR intracellular tail (residues 780–860) cloned into pACT2-DEST, and PJ69-4a transformed with the bait constructs cloned into pGDBU-DEST were selected on minimal agar plates lacking leucine or uracil, respectively. For mating, cells were precultured for 16 hours in selection medium, and subsequently 2 $\times$ 10<sup>6</sup> of transformed PJ69-4a and PJ69-4 $\alpha$  cells were mated in 2 $\times$ YPAD for 24 hours with slow shaking. Diploids were selected on minimal glucose plates lacking both leucine and uracil. To reconfirm interactions, we used a spot assay. Briefly, diploid cells were incubated for 16 hours in minimal glucose medium lacking leucine and uracil, diluted to OD<sub>600</sub> of 0.2 and grown till an OD<sub>600</sub> of 1. Cells were then serially diluted so as to plate 10<sup>2</sup>–10<sup>5</sup> cells/spot on minimal glucose agar lacking leucine and uracil, with or without histidine, 10 to 20 mmol/L 3-aminotriazol, and adenine. Plates were incubated for 3 days before analysis.

## Statistical Analysis

Data are presented as mean $\pm$ SD. One-way ANOVA followed by the Bonferroni correction was performed for comparison of >2 groups. Student's *t* test was performed for comparison of 2 groups. *P* values of <0.05 were considered significant.

## Results

### USP2 Is a Novel-Binding Partner of IDOL

The LDLR is a constitutive recycling receptor that rapidly shuttles between the plasma membrane and endosomal compartments. Internalization of the receptor is a clathrin-dependent process that requires adaptor proteins yet does not involve receptor ubiquitylation.<sup>3</sup> Next to the classical LDLR pathway, IDOL-stimulated ubiquitylation of the receptor promotes internalization of the receptor via a distinct, clathrin-independent endocytic route that requires activity of the endosomal-sorting complex required for transport–associated deubiquitylase USP8.<sup>6,7</sup> As strategies to increase abundance of the LDLR form the cornerstone of current therapies of hypercholesterolemia, we hypothesized that other deubiquitylases might counteract IDOL-mediated ubiquitylation and degradation of the LDLR, and thus regulate LDL metabolism.

To uncover deubiquitylases potentially involved in the regulation of the IDOL–LDLR network, we used a biased yeast-2-hybrid approach aimed at identifying deubiquitylases interacting with IDOL, or alternatively with the intracellular tail of the LDLR. The latter contains the structural and functional requirements for internalization, sorting, and ubiquitylation of the LDLR.<sup>3,22</sup> Our prey library contained 61 deubiquitylases, representing 77% of known active mammalian deubiquitylases, previously used in a systematic deubiquitylase–E3 interaction screen (Online Table I).<sup>20</sup> This screen failed to identify any LDLR-tail-interacting deubiquitylases (Online Figure IA). However, the assay identified

the deubiquitylase USP2-69 isoform (referred to further as USP2), as an interacting partner of the full-length IDOL protein (Online Table I). IDOL contains 2 functional regions, a FERM and a RING domain, which are joined by a short linker (Figure 1A). Using the yeast-2-hybrid assay, we mapped IDOL's F3 and linker subdomains as the minimal regions required for interacting with USP2 (Figure 1A and 1B; Online Figure IB). Importantly, the interaction with USP2 was also maintained with a severe IDOL RING mutant, IDOL<sub>C387A</sub>. This mutation disrupts the conserved RING structure and as a result this mutant is unable to promote LDLR degradation and to support IDOL autoubiquitylation,<sup>8</sup> suggesting that both functions are not essential for the physical interaction of USP2 and IDOL. Furthermore, this result also indicates that USP2 does not compete with binding of the E2-ligase to IDOL, an interaction that depends on an intact RING domain.<sup>22,26</sup> We next confirmed that this interaction also takes place in mammalian cells (HEK293T). Immunoprecipitation of transfected USP2 or IDOL (1:1 ratio) resulted in copurification of the corresponding binding partner (Figure 1C; Online Figure IIA). Furthermore, the interaction with IDOL was independent of USP2s catalytic activity because it was maintained in the USP2<sub>C276A</sub> catalytic mutant (Online Figure IIB). In addition to USP2-69 identified in our yeast-2-hybrid screen, a shorter isoform of USP2, USP2-45, has been also described.<sup>27</sup> These 2 USP2 isoforms differ in their N-terminal region and tissue distribution, but share the common C-terminal catalytic domain (Online Figure IIC). Like the USP2-69 isoform, the lower-molecular weight isoform, USP2-45 interacted with IDOL as well (Figure 1D). This points to the catalytic C-terminal region of USP2 as the IDOL interacting region, which is the same region implicated in the interaction of USP2 with the E3 MDM2.<sup>28</sup> Taken together, these results identify USP2 as a novel-binding partner of IDOL and as a potential regulatory component of the IDOL–LDLR axis.

### USP2 Deubiquitylates and Stabilizes IDOL

To study the functional consequence of the USP2–IDOL interaction, we initially used a gain-of-function approach. Remarkably, we found that overexpression of USP2 markedly stabilized IDOL protein (Figure 2A). USP8 however failed to do so, supporting the notion that the antagonizing effects of USP8 on the LXR–IDOL–LDLR axis occur primarily at the level of the ubiquitylated receptor. The stabilization of wild-type IDOL was equivalent to that observed with the proteasome inhibitor MG132, and required USP2 catalytic activity, as it was not seen with USP2<sub>C276A</sub> (Figure 2B). Thus, in spite of the preserved interaction of IDOL with both wild-type USP2 and USP2<sub>C276A</sub>, only the active form of USP2 could increase IDOL levels. This finding implies that the deubiquitylase activity of USP2, rather than steric hindrance is required for IDOL stabilization. We have previously reported that IDOL is a highly unstable protein, likely because of its high autoubiquitylation activity.<sup>8</sup> Accordingly, using cycloheximide to prevent protein synthesis we could determine that stabilization of IDOL by USP2 was a result of the extension of IDOL's half-life (Figure 2C; Online Figure III). The most parsimonious explanation for this observation is that IDOL is subject to USP2-mediated deubiquitylation, which

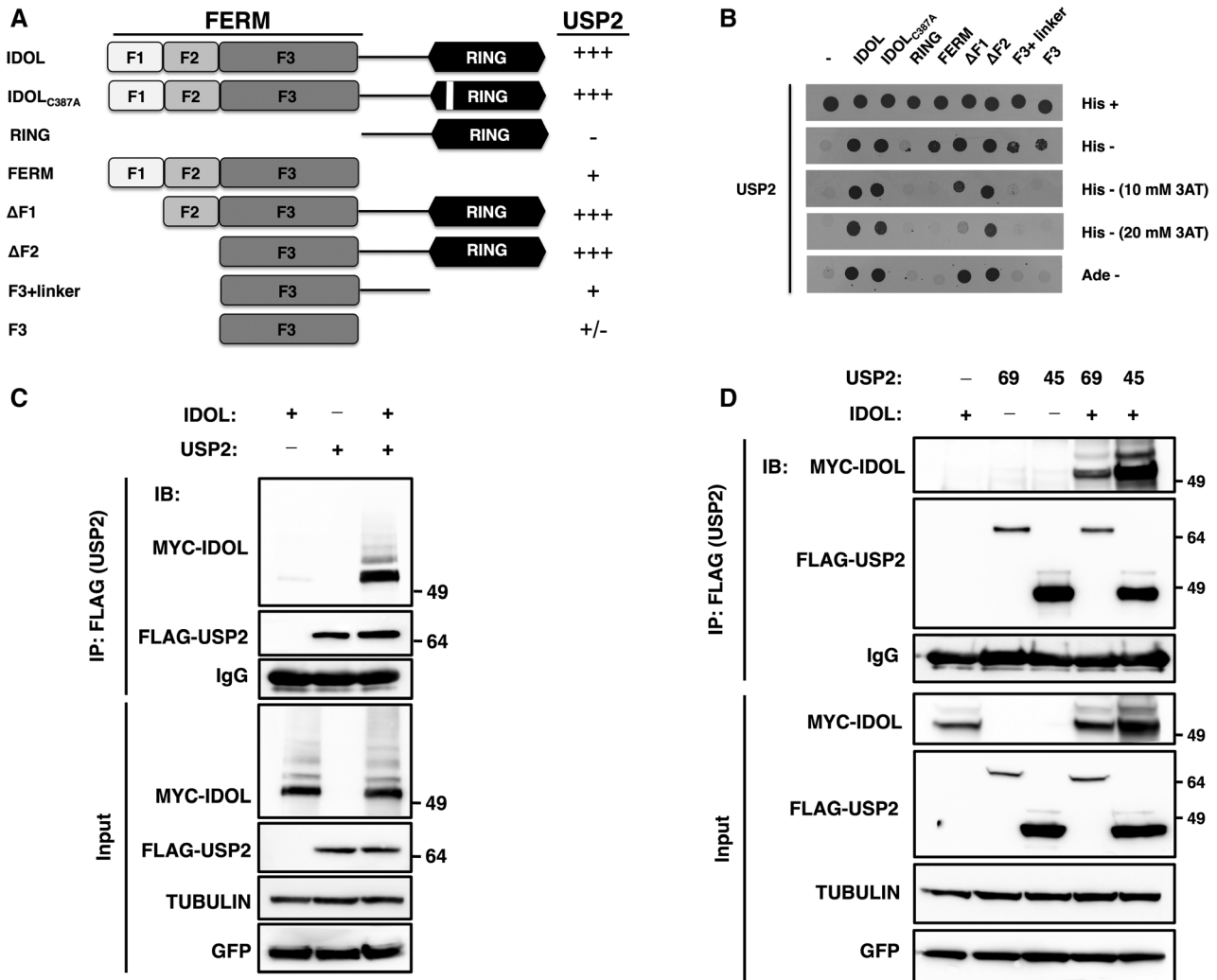


**Figure 1. The deubiquitylase ubiquitin-specific protease 2 (USP2) is a novel-binding partner of inducible degrader of the low-density lipoprotein receptor (IDOL).** **A**, Representation of the IDOL-USP2 interaction assay in yeast. IDOL contains an N-terminal FERM domain and a C-terminal RING domain separated by a short linker region. The FERM contains the 3 subdomains, F1, F2, and F3, found in other FERM-containing proteins. A semiquantitative score for the interaction of the IDOL constructs with USP2, based on the growth of the yeast colonies, is reported on the right (+++=strong interaction, -=no interaction). **B**, The different IDOL fragments shown in (A) and USP2 were cloned into yeast-2-hybrid prey and bait plasmids and transformed into yeast. Haploid cells were mated, and diploid cells were serially diluted and plated on selective plates. An image from the first serial dilution ( $10^5$  diploids plated) is shown. **C** and **D**, HEK293T cells were transfected with the indicated expression constructs for IDOL, USP2-69, and USP2-45 (IDOL:USP2 ratio of 1:1-3). Total cell lysates were immunoblotted or immunoprecipitated and analyzed as indicated. All immunoblots are representative of at least 3 independent experiments.

prevents its degradation. To test this, we conducted experiments in conjunction with pharmacological blocking of proteasomal degradation. This treatment equalizes IDOL levels and promotes accumulation of ubiquitylated IDOL species. Under this condition, both USP2 isoforms reduced the degree of ubiquitylated IDOL (Figure 2D and 2E). Furthermore, consistent with the lack of IDOL stabilization by the catalytic mutant USP2<sub>C276A</sub> or by USP8, we observed no changes in the degree of IDOL ubiquitylation by these deubiquitylases. If USP2 removes ubiquitin from IDOL and promotes its stability, the opposite can be expected if USP2 is silenced. Unfortunately, we cannot determine the endogenous level of IDOL in cells, as no commercial or homemade antibodies are able to detect it (data not shown). For that reason, we transfected IDOL into hepatocyte-like human HepG2 and Huh7

cells, and determined the level of heterologous IDOL protein after silencing USP2 expression. We observed that effective silencing of USP2 in these cells ( $55\pm 6\%$  reduction) reduced immunodetectable IDOL protein (Online Figure IVA and IVB), consistent with the notion that USP2 removes ubiquitin from IDOL to prevent its degradation. Thus, our experiments demonstrate that both gain and loss of USP2 function modulate the level of IDOL protein.

**USP2 Counteracts IDOL-Mediated Degradation of the LDLR**

In view of these findings, we predicted that USP2 would promote degradation of the LDLR because of increased IDOL abundance. However, unexpectedly we observed the opposite outcome. Despite massive stabilization of IDOL,

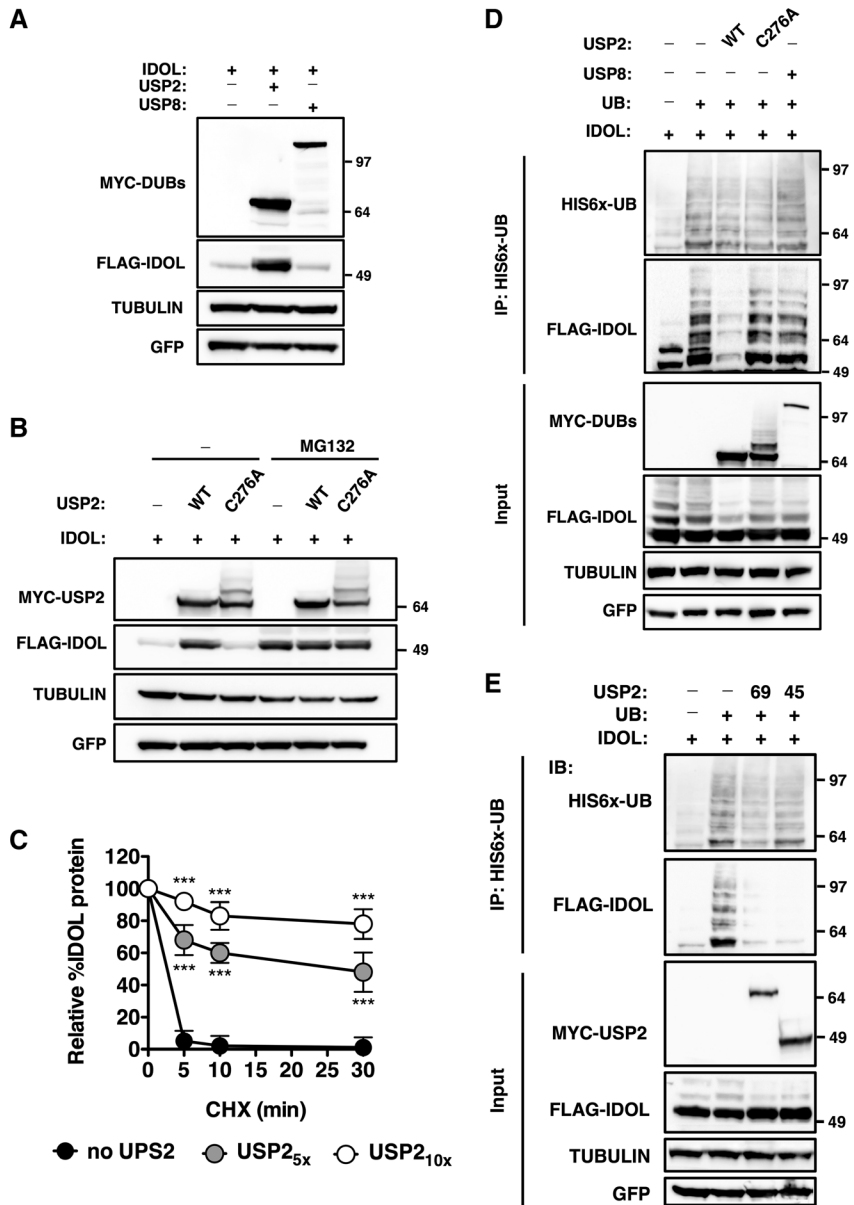


**Figure 2. Ubiquitin-specific protease 2 (USP2) deubiquitylates inducible degrader of the low-density lipoprotein receptor (IDOL) and increases its stability.** **A**, HEK293T cells were transfected with the indicated expression constructs for IDOL, USP2, and USP8 (at a IDOL:DUB ratio of 1:3) and total cell lysates were immunoblotted as indicated. **B**, HEK293T cells were transfected with the indicated expression constructs for IDOL, USP2 wild-type (WT), or the USP2 catalytic mutant. Forty-eight hours after transfection, cells were treated with 25 μmol/L MG132 for 6 hours and collected for analysis. Total cell lysates were immunoblotted as indicated. **C**, HEK293T cells were transfected with IDOL (black circle) or together with USP2 expression vectors at a 1:5 (gray circle) or 1:10 (white circle) ratio. Forty-eight hours after transfection, cells were incubated for the indicated times with 10 μg/mL cycloheximide (CHX), and cells harvested for immunoblots analysis (n=3, \*\*\*P<0.001). **D** and **E**, HEK293T cells were transfected with the indicated expression constructs for IDOL, USP8, USP2-69 WT or catalytic mutant, USP2-45 and Ubiquitin. Forty-eight hours after transfection, cells were treated with 25 μmol/L MG132 for 6 hours and collected for analysis. Total cell lysates were immunoblotted or immunoprecipitated and analyzed as indicated. All immunoblots are representative of at least 3 independent experiments.

USP2 (-69 and -45) prevented degradation of the LDLR, as well as of a second IDOL target, the very low-density lipoprotein receptor,<sup>29</sup> in a dose- and activity-dependent fashion (Figure 3A–3C; Online Figure VA). Because *IDOL* is a transcriptional target of LXR,<sup>8</sup> and LXR-induced degradation of the LDLR is IDOL-dependent,<sup>30</sup> we also evaluated whether USP2 can counteract the effect of LXR on the LDLR. In agreement with our findings, USP2 was also able to counteract LXR-induced LDLR degradation, even though expression of *IDOL* was induced (Online Figure VB and VC). We also considered the possibility that expression of *USP2* is sensitive to the cellular sterol status. However, we found that neither LXR activation nor variation of the cellular sterol content altered *USP2* expression (Online Figure VD). Functionally, antagonism of IDOL activity by USP2 counteracted the decrease in cellular LDL uptake imposed by IDOL (Figure 3D), positioning this deubiquitylase as a potential regulator of lipoprotein uptake.

### Silencing USP2 Promotes LDLR Degradation in an IDOL-Dependent Manner

To understand how USP2 counters the IDOL–LDLR nexus, we tested the consequence of silencing *USP2* on the LDLR pathway in hepatic and nonhepatic cell lines. These cells express *IDOL* and are, therefore, suitable for studying the functional interaction between IDOL and USP2 (Online Figure VIA). Silencing of *USP2* in these cells led to a marked reduction in LDLR protein without changing the level of *LDLR* mRNA (Figure 4A and 4B; Online Figure VIB–VID). The secreted protein PCSK9 promotes degradation of the LDLR, and it is expressed by HepG2 cells.<sup>31</sup> It was therefore conceivable that silencing *USP2* increases *PCSK9* expression, and that this, in turn, leads to LDLR degradation. However, this does not seem to be the case because in HepG2 cells, *PCSK9* expression was not sensitive to the level of USP2 (Figure 4B). In contrast to the effects of silencing *USP2* on the LDLR, another membrane receptor, the epidermal growth factor receptor (EGFR), remained either

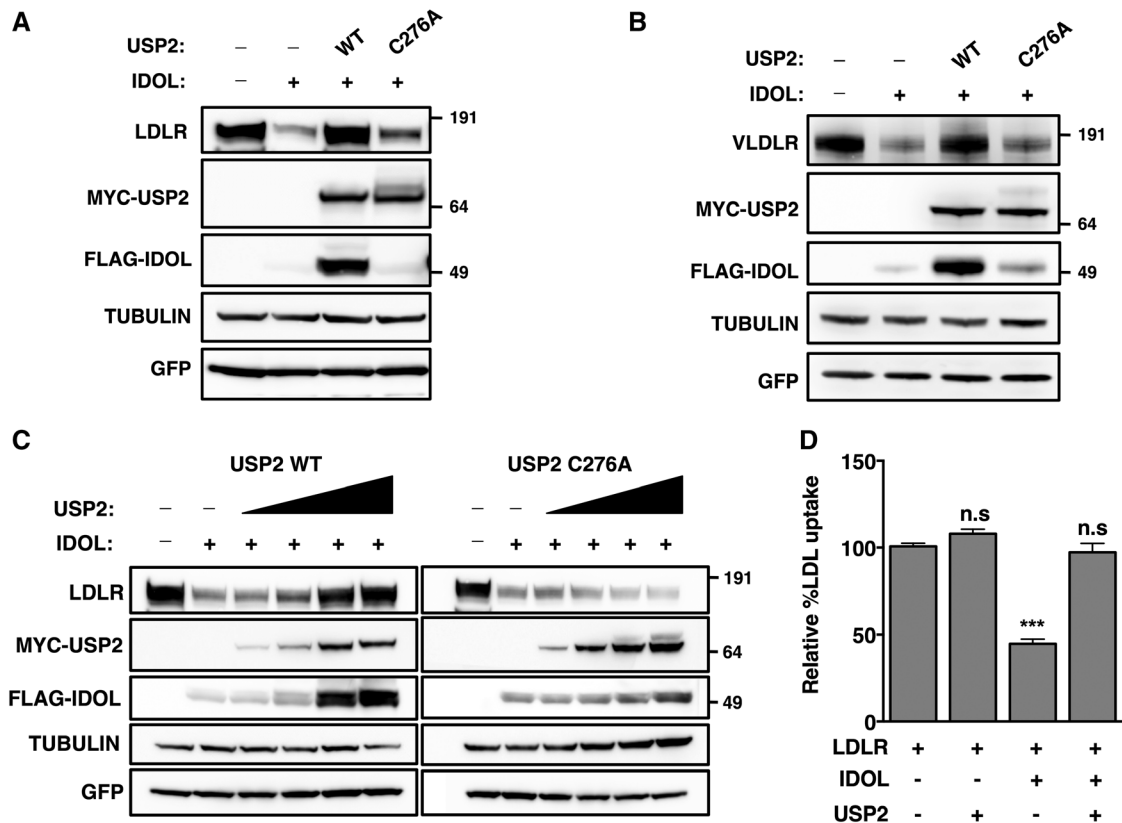


**Figure 3. Ubiquitin-specific protease 2 (USP2) antagonizes the inducible degrader of the low-density lipoprotein (LDL) receptor (IDOL)-mediated degradation of lipoprotein receptors.** **A** and **B**, HEK293T cells were transfected with expression constructs encoding FLAG-IDOL, LDL receptor (LDLR) (**A**) or very low-density lipoprotein receptor (VLDLR)-HA; (**B**), and MYC-USP2 wild-type (WT) or catalytic mutant as indicated. Forty-eight hours after transfection cells were collected and total cell lysates immunoblotted as indicated. **C**, HEK293T cells were transfected with the indicated LDLR, IDOL, and USP2 expression vectors, with increasing amounts of WT or mutant USP2. Forty-eight hours after transfection, cells were harvested for immunoblots analysis as shown (**D**). HEK293T cells were transfected with expression constructs encoding FLAG-IDOL, LDLR, and MYC-USP2 WT. Twenty-four hours after transfection, cells were incubated for 30 minutes with 5  $\mu$ g/mL Dylight 488-labeled LDL. After extensive washing, internalized LDL was quantified by measuring fluorescence in cell lysates. LDL uptake in cells not expressing IDOL and USP2 was set to 100%. Each bar and error represent the average $\pm$ SD ( $n=8$ , \*\*\* $P<0.0001$ ). All immunoblots are representative of at least 3 independent experiments.

unchanged or even slightly increased after knockdown of *USP2* in these cells (Figure 4A; Online Figure VIB). Unfortunately, we were unable to detect endogenous USP2 with commercially available antibodies in our experimental assays (not shown). Therefore, to establish the specificity of our USP2 siRNA and to rule out off target effects, we tested 3 individual USP2 siRNAs. All the 3 effectively knocked down expression of *USP2* in HepG2 cells and decreased the protein levels of the LDLR (Online Figure VIIA and VIIB). Consistent with IDOL targeting an LDLR pool present at the plasma membrane,<sup>6,7</sup> we found that silencing *USP2* resulted in prominent removal of LDLR from the cell surface ( $100\pm 2.6$  in control versus  $30.4\pm 4.9$  in siUSP2,  $n=8$ ,  $P<0.0001$ ; Figure 4C), and as a consequence attenuated LDL uptake in different cell types (Figure 4D). Having established that USP2 influences the level of LDLR protein, we now asked if this mechanism requires IDOL activity. To test this, we silenced *Usp2* in wild-type or *Idol*<sup>-/-</sup> MEFs (Figure 4E; Online Figure VIE). Effective silencing of *Usp2* in wild-type cells decreased the LDLR. In *Idol*<sup>-/-</sup> cells LDLR protein was elevated, as previously reported,<sup>30</sup> yet was insensitive to loss of *Usp2*. Collectively, these results demonstrate the functional importance of the USP2-IDOL nexus in physiological control of LDLR levels.

### IDOL, USP2, and the LDLR Form a Functional Tri-Partite Complex to Regulate LDLR Ubiquitylation and Degradation

Our results demonstrate that USP2 can control LDLR protein abundance in an IDOL-dependent manner. Yet this raises a paradox; whereas USP2 dramatically stabilizes IDOL by promoting its deubiquitylation, it also inhibits IDOL-stimulated degradation of the LDLR. Conversely, silencing of *USP2* decreases IDOL protein yet enhances degradation of the LDLR. To untangle this conundrum, we set out to test the requirements for interaction between IDOL, USP2, and the LDLR, and to determine the consequence of these interactions on ubiquitylation and degradation of the receptor. First, because USP2 can reverse IDOL-mediated degradation of the LDLR, we wanted to test whether elevating the level of USP2 influences ectopic LDLR levels independent of IDOL (Figure 5A). We introduced USP2 into cells at an increasing dose but found that this had no effect on LDLR protein, unlike what we observed in the presence of IDOL (Figure 3). This suggests that for USP2 to modulate LDLR levels, ubiquitylation of the receptor is required. In the yeast-2-hybrid screen, no interaction between USP2 and the intracellular tail of the LDLR was detected (Online Figure IA). Yet, in this assay it is likely that the

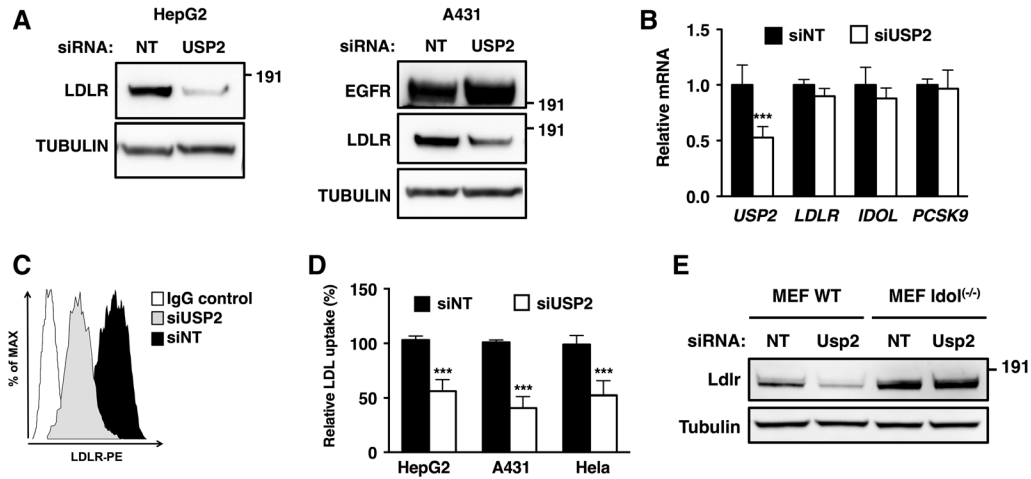


**Figure 4. Silencing ubiquitin-specific protease 2 (USP2) promotes low-density lipoprotein receptor (LDLR) degradation in an inducible degrader of the LDL receptor (IDOL)-dependent manner.** **A**, HepG2 and A431 cells were cultured for 16 hours in sterol-depletion medium to induce LDLR. Subsequently, cells were transfected as indicated with control (nontargeting [NT]) or *USP2* siRNA. Seventy-two hours after transfection, cells were collected and analyzed by immunoblotting. **B**, HepG2 were cultured and treated as in **A** and analyzed by quantitative polymerase chain reaction (n=4, \*\*\**P*<0.01). **C**, A431 cells were cultured and treated as in **A**, and LDLR at the cell surface was determined by fluorescence-activated cell sorter. **D**, HepG2, A431, and HeLa cells were cultured and treated as in **A** and **B**. Seventy-two hours after transfection, cells were incubated for 30 minutes with 5 μg/mL Dylight 488-labeled LDL. After extensive washing, internalized LDL was quantified by measuring fluorescence in cell lysates. LDL uptake in control cells was set to 100%. Each bar and error represent the average±SD (n=4, \*\*\**P*<0.001). **E**, Wild-type (WT) and *Idol*<sup>(-/-)</sup> mouse embryonic fibroblasts (MEFs) were cultured and treated as in **A** and **B**. Seventy-two hours after transfection, cells were collected and analyzed by immunoblotting. All immunoblots are representative of at least 3 independent experiments.

tail is not ubiquitylated because yeast do not encode an IDOL homolog, and in this assay the tail is presented out of its normal, membrane-linked context. Therefore, we tested whether USP2 interacts with the LDLR in mammalian cells, and found that USP2 could be pulled down with the LDLR, albeit weakly (Figure 5B, lane 4). We specifically chose to use the FERM domain in these experiments because the FERM domain binds USP2, and it is recruited to, and binds the LDLR at the plasma membrane,<sup>22</sup> but does not stimulate degradation of the receptor because of the lack of the RING domain. As expected, the FERM domain interacted with the LDLR (Figure 5B, lane 7). Yet when all the 3 were introduced into cells, we found

that both USP2 and IDOL were readily coimmunoprecipitated with the LDLR (Figure 5B, lane 8). This result supports the idea that a tri-partite complex, containing IDOL, USP2, and the LDLR is formed at the plasma membrane. To capture this complex, we used overexpression of the endocytic adaptor molecule Epsin1, which acts in a dominant negative manner to block Epsin1-dependent endocytosis. We have previously used this approach to demonstrate that it effectively blocks IDOL-stimulated degradation of the LDLR.<sup>6</sup> This is because of Epsin1 blocking internalization of the LDLR following IDOL-mediated ubiquitylation, thus resulting in accumulation of ubiquitylated LDLR at the plasma membrane. As

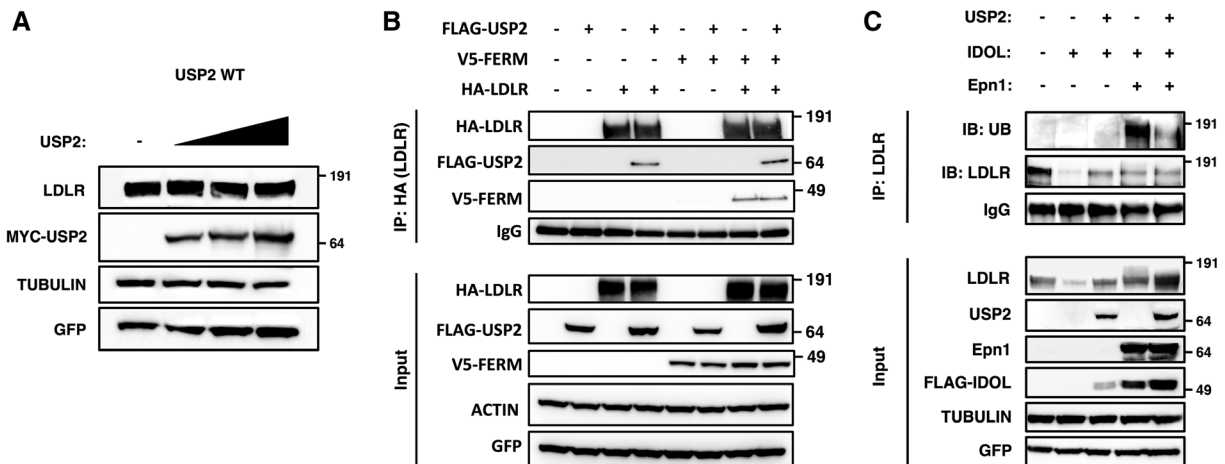


**Figure 5. Inducible degrader of the low-density lipoprotein receptor (IDOL), ubiquitin-specific protease 2 (USP2), and the LDLR form a functional tri-partite complex to regulate LDL receptor (LDLR) ubiquitylation and degradation.** **A**, **B**, and **C**, HEK293T cells were transfected with (A) LDLR and increased amounts of USP2-69 expression plasmids, (B) HA-LDLR, USP2-69, and IDOL<sup>FERM</sup> expression plasmids, and (C) LDLR, Epsin, IDOL, and USP2. Forty-eight hours after transfection, total cell lysates were immunoblotted or immunoprecipitated and analyzed as indicated. All immunoblots are representative of at least 3 independent experiments. WT indicates wild-type.

shown, both Epsin1 and USP2 could block IDOL-dependent degradation of the receptor (Figure 5C, lanes 1–4). The use of dominant negative Epsin1 also increased ubiquitylated LDLR species, as expected. Yet when the deubiquitylase USP2 was also present, the level of ubiquitylated LDLR was markedly reduced (Figure 5C, lane 5). Collectively, these experiments support the notion that USP2 can counteract IDOL-dependent ubiquitylation of the LDLR, and prevent the receptor from being directed toward lysosomal degradation.

## Discussion

The LDLR provides the main entry portal for LDL into the cell, and the mechanisms characterizing its transcriptional regulation and endocytic network have been largely described.<sup>3,4</sup> Recently, the ubiquitin-proteasome system (UPS) was recognized as a novel regulatory layer in the LDLR pathway through the discovery of ubiquitylation-dependent degradation of the LDLR, mediated by the E3-ubiquitin ligase IDOL.<sup>8</sup> IDOL stimulates clathrin-independent internalization and lysosomal degradation of the LDLR, a process requiring sorting of the ubiquitylated receptor by the endosomal-sorting complex required for transport system.<sup>6,7,13</sup> The main finding of this study is the identification of USP2 as a deubiquitylase counteracting IDOL activity, and as a consequence abundance of the LDLR.

In view of the reversible nature of ubiquitylation, we reasoned that deubiquitylases counteracting IDOL activity might exist. To investigate this, we screened IDOL and the intracellular tail of the LDLR for potential interactions with a representative collection of human deubiquitylases. The screen with the LDLR intracellular tail failed to identify any LDLR-interacting deubiquitylases. This was somewhat surprising as previous studies, ours included, reported that USP8 is essential for IDOL-mediated degradation of the LDLR,<sup>6,7</sup> and USP8 was included in our deubiquitylase screen. This apparent incongruence is possibly because of the fact that the cytosolic LDLR tail is only recognized by USP8 when ubiquitylated and in the context of a biological membrane, and not in the native form that is likely the one prevalent in the yeast-2-hybrid assay. However, by screening the deubiquitylase library against IDOL, we identified USP2 as a novel IDOL-binding protein. Our biochemical and molecular-based findings collectively indicate that USP2 interacts with IDOL and significantly increases its lifespan. The increased stabilization of IDOL is a result of its USP2-dependent deubiquitylation, similar to what has been described for the USP2–MDM2 and USP2–MDMX complexes.<sup>28,32</sup> Regulation of E3 ligases by deubiquitylase-mediated deubiquitylation has been previously reported and represents an emerging concept in E3 control.<sup>17,19–21</sup> Previous reports indicated that deubiquitylases stabilize E3s by limiting their autoubiquitylation. Consequently, deubiquitylation of E3s acts to enhance substrate ubiquitylation. In line with this, USP2 deubiquitylates and stabilizes MDM2 and ITC, which results in increased ubiquitylation and degradation of their cognate substrates.<sup>28,33</sup> In contrast to this model, deubiquitylation of IDOL by USP2 leads to a paradoxical outcome in which increased levels of the E3 ligase are mirrored by decreased degradation of its targets (ie, the LDLR and very low-density lipoprotein receptor) and functionally leads to

enhanced cellular LDL uptake. In line with this, silencing of *USP2* accelerates LDLR degradation and decreases LDL uptake in an IDOL-dependent manner in a variety of cell types.

Our results suggest that IDOL, USP2, and the LDLR form a tri-partite complex at the plasma membrane, and in that context ubiquitylation of the receptor is decreased. The most plausible scenario to explain this outcome is that IDOL-mediated ubiquitylation of the LDLR is counteracted by subsequent removal of ubiquitin chains from the LDLR by USP2. In this sequential scenario, USP2 is recruited by IDOL and acts directly on the receptor, reminiscent of the reported effect of USP2 on EGFR after ligand binding.<sup>34</sup> This would be consistent with the fact that the phenotype is IDOL dependent, and that USP2 is able to process diverse ubiquitin linkages.<sup>35,36</sup> Although we think this is the probable scenario, our experiments cannot formally rule out a more provocative possibility, namely that ubiquitylation of IDOL itself serves to both regulate its stability (ie, autoubiquitylation) and activity (ie, LDLR ubiquitylation). As such, by removing ubiquitin from IDOL, USP2 could counteract both processes. Although speculative, this form of regulation is not without precedent.<sup>37–39</sup> Both *cis* and *trans* ubiquitylation of E3 ligases has been reported, and we have observed that USP2 can remove ubiquitin chains from an IDOL mutant lacking autoubiquitylation activity (data not shown). The significance of this observation requires further investigation, yet it is possible that these modifications may allow a hierarchical E3-based network for fine tuning of cellular proteostasis.<sup>19,40</sup>

The role of USP2 in regulating the IDOL–LDLR pathway seems to be exclusively dependent on post-transcriptional events because *USP2* expression is unaffected by perturbing the cellular sterol content or by pharmacologically activating LXR in different cell types. Therefore, identifying the signals, or post-transcriptional modifications on USP2 or IDOL that regulate their functional interaction will be an important goal in future studies. The *USP2* gene is alternatively spliced into 3 isoforms,<sup>27</sup> all sharing an identical C-terminal catalytic core. The 2 major USP2 isoforms, USP2-69 and USP2-45, promote IDOL deubiquitylation and rescue LDLR degradation. The specific functions and regulation of these 2 distinct isoforms are not well understood. The *USP2-69* isoform is induced by androgens both in human and in rat prostate cells<sup>41</sup> and by the AKT–mTORC1 axis in hepatocellular carcinoma.<sup>42</sup> The mouse *Usp2-45* isoform is regulated by the transcriptional coactivator PGC-1 $\alpha$ , which couples the circadian and nutritional control in the liver in response to starvation.<sup>43</sup> The above-mentioned regulation suggests that expression of *USP2* is sensitive to nutritional and circadian input. Given that cholesterol metabolism is subject to these cues as well, it will be important to investigate how USP2 is integrated with the IDOL–LDLR axis *in vivo*. We speculate that the functional interaction between USP2 and IDOL, and the formation of a tri-partite complex with the LDLR, may be sensitive to post-transcriptional modifications, nutritional cues, or to the dynamic levels of these proteins. However, a serious limitation in experimentally testing the physiological role of the USP2–IDOL nexus is the species-dependent differences in hepatic IDOL activity and transcriptional regulation<sup>12</sup>; whereas in human and in nonhuman primates, the IDOL pathway is highly active in

hepatocytes and subject to strong sterol-dependent transcriptional regulation, in rodent hepatocytes it is not. Accordingly, *Idol*<sup>(-/-)</sup> mice do not display a marked cholesterol phenotype or changes in hepatic LDLR content. We therefore anticipate that a functional USP2–IDOL interaction will be predominantly active in human hepatocytes. In that respect, the growing body of evidence pointing toward genetic variation in *IDOL* as a modifier of LDL cholesterol in humans,<sup>9–11</sup> warrants further studies to investigate the basic mechanisms governing IDOL activity and regulation by USP2.

In summary, this study reports the identification of the deubiquitylase USP2 as an endogenous inhibitor of IDOL and a novel modulator of lipoprotein uptake owing to its ability to counteract IDOL-stimulated degradation of the LDLR (graphically summarized in Online Figure VIII). This finding further supports the notion that inhibition of IDOL activity would result in increased LDLR abundance and enhance LDL uptake, an approach that can be exploited as a therapeutic strategy to treat dyslipidemia and coronary artery disease.

### Acknowledgments

We acknowledge members of the Zelcer group, Menno de Winter and Irith Koster for their comments and suggestions.

### Sources of Funding

B. Distel is supported by a TOP grant (91209046) from the Netherlands Organization of Scientific Research (NWO). N. Zelcer is an Established Investigator of the Dutch Heart Foundation (2013T111), and he is supported by a VIDI grant (17.106.355) from the Netherlands Organization of Scientific Research (NWO), and by a European Research Council (ERC) Consolidator grant (617376) from the European Research Council.

### Disclosures

None.

### References

- Hobbs HH, Russell DW, Brown MS, Goldstein JL. The LDL receptor locus in familial hypercholesterolemia: mutational analysis of a membrane protein. *Annu Rev Genet.* 1990;24:133–170. doi: 10.1146/annurev.gen.24.120190.001025.
- Tolleshaug H, Goldstein JL, Schneider WJ, Brown MS. Posttranslational processing of the LDL receptor and its genetic disruption in familial hypercholesterolemia. *Cell.* 1982;30:715–724.
- Brown MS, Goldstein JL. A receptor-mediated pathway for cholesterol homeostasis. *Science.* 1986;232:34–47.
- Horton JD, Goldstein JL, Brown MS. SREBPs: activators of the complete program of cholesterol and fatty acid synthesis in the liver. *J Clin Invest.* 2002;109:1125–1131. doi: 10.1172/JCI15593.
- Goldstein JL, Brown MS. The LDL receptor. *Arterioscler Thromb Vasc Biol.* 2009;29:431–438. doi: 10.1161/ATVBAHA.108.179564.
- Sorrentino V, Nelson JK, Maspero E, Marques AR, Scheer L, Polo S, Zelcer N. The LXR-IDOL axis defines a clathrin-, caveolae-, and dynamin-independent endocytic route for LDLR internalization and lysosomal degradation. *J Lipid Res.* 2013;54:2174–2184. doi: 10.1194/jlr.M037713.
- Scotti E, Calamai M, Goulbourne CN, Zhang L, Hong C, Lin RR, Choi J, Pilch PF, Fong LG, Zou P, Ting AY, Pavone FS, Young SG, Tontonoz P. IDOL stimulates clathrin-independent endocytosis and multivesicular body-mediated lysosomal degradation of the low-density lipoprotein receptor. *Mol Cell Biol.* 2013;33:1503–1514. doi: 10.1128/MCB.01716-12.
- Zelcer N, Hong C, Boyadjian R, Tontonoz P. LXR regulates cholesterol uptake through Idol-dependent ubiquitination of the LDL receptor. *Science.* 2009;325:100–104. doi: 10.1126/science.1168974.
- Teslovich TM, Musunuru K, Smith AV, et al. Biological, clinical and population relevance of 95 loci for blood lipids. *Nature.* 2010;466:707–713. doi: 10.1038/nature09270.
- Chasman DI, Paré G, Mora S, Hopewell JC, Peloso G, Clarke R, Cupples LA, Hamsten A, Kathiresan S, Mälarstig A, Ordovas JM, Ripatti S, Parker AN, Miletich JP, Ridker PM. Forty-three loci associated with plasma lipoprotein size, concentration, and cholesterol content in genome-wide analysis. *PLoS Genet.* 2009;5:e1000730. doi: 10.1371/journal.pgen.1000730.
- Sorrentino V, Fouchier SW, Motazacker MM, Nelson JK, Defesche JC, Dallinga-Thie GM, Kastelein JJ, Kees Hovingh G, Zelcer N. Identification of a loss-of-function inducible degrader of the low-density lipoprotein receptor variant in individuals with low circulating low-density lipoprotein. *Eur Heart J.* 2013;34:1292–1297. doi: 10.1093/eurheartj/ehs472.
- Hong C, Marshall SM, McDaniel AL, et al. The LXR-Idol axis differentially regulates plasma LDL levels in primates and mice. *Cell Metab.* 2014;20:910–918. doi: 10.1016/j.cmet.2014.10.001.
- Sorrentino V, Zelcer N. Post-transcriptional regulation of lipoprotein receptors by the E3-ubiquitin ligase inducible degrader of the low-density lipoprotein receptor. *Curr Opin Lipidol.* 2012;23:213–219. doi: 10.1097/MOL.0b013e3283532947.
- Sharpe LJ, Cook EC, Zelcer N, Brown AJ. The UPS and downs of cholesterol homeostasis. *Trends Biochem Sci.* 2014;39:527–535. doi: 10.1016/j.tibs.2014.08.008.
- Reyes-Turcu FE, Ventii KH, Wilkinson KD. Regulation and cellular roles of ubiquitin-specific deubiquitinating enzymes. *Annu Rev Biochem.* 2009;78:363–397. doi: 10.1146/annurev.biochem.78.082307.091526.
- Sowa ME, Bennett EJ, Gygi SP, Harper JW. Defining the human deubiquitinating enzyme interaction landscape. *Cell.* 2009;138:389–403. doi: 10.1016/j.cell.2009.04.042.
- Komander D, Clague MJ, Urbé S. Breaking the chains: structure and function of the deubiquitinases. *Nat Rev Mol Cell Biol.* 2009;10:550–563. doi: 10.1038/nrm2731.
- Ventii KH, Wilkinson KD. Protein partners of deubiquitinating enzymes. *Biochem J.* 2008;414:161–175. doi: 10.1042/BJ20080798.
- de Bie P, Ciechanover A. Ubiquitination of E3 ligases: self-regulation of the ubiquitin system via proteolytic and non-proteolytic mechanisms. *Cell Death Differ.* 2011;18:1393–1402. doi: 10.1038/cdd.2011.16.
- Hayes SD, Liu H, MacDonald E, Sanderson CM, Coulson JM, Clague MJ, Urbé S. Direct and indirect control of mitogen-activated protein kinase pathway-associated components, BRAP/IMP E3 ubiquitin ligase and CRAF/RAF1 kinase, by the deubiquitylating enzyme USP15. *J Biol Chem.* 2012;287:43007–43018. doi: 10.1074/jbc.M112.386938.
- Clague MJ, Coulson JM, Urbé S. Cellular functions of the DUBs. *J Cell Sci.* 2012;125:277–286. doi: 10.1242/jcs.090985.
- Sorrentino V, Scheer L, Santos A, Reits E, Bleijlevens B, Zelcer N. Distinct functional domains contribute to degradation of the low density lipoprotein receptor (LDLR) by the E3 ubiquitin ligase inducible Degradator of the LDLR (IDOL). *J Biol Chem.* 2011;286:30190–30199. doi: 10.1074/jbc.M111.249557.
- Shan J, Zhao W, Gu W. Suppression of cancer cell growth by promoting cyclin D1 degradation. *Mol Cell.* 2009;36:469–476. doi: 10.1016/j.molcel.2009.10.018.
- Oh KH, Yang SW, Park JM, Seol JH, Iemura S, Natsume T, Murata S, Tanaka K, Jeon YJ, Chung CH. Control of AIF-mediated cell death by antagonistic functions of CHIP ubiquitin E3 ligase and USP2 deubiquitinating enzyme. *Cell Death Differ.* 2011;18:1326–1336. doi: 10.1038/cdd.2011.3.
- Motazacker MM, Pirruccello J, Huijgen R, Do R, Gabriel S, Peter J, Kuivenhoven JA, Defesche JC, Kastelein JJ, Hovingh GK, Zelcer N, Kathiresan S, Fouchier SW. Advances in genetics show the need for extending screening strategies for autosomal dominant hypercholesterolemia. *Eur Heart J.* 2012;33:1360–1366. doi: 10.1093/eurheartj/ehs010.
- Zhang L, Fairall L, Goult BT, Calkin AC, Hong C, Millard CJ, Tontonoz P, Schwabe JW. The IDOL-UBE2D complex mediates sterol-dependent degradation of the LDL receptor. *Genes Dev.* 2011;25:1262–1274. doi: 10.1101/gad.2056211.
- Gousseva N, Baker RT. Gene structure, alternate splicing, tissue distribution, cellular localization, and developmental expression pattern of mouse deubiquitinating enzyme isoforms Usp2-45 and Usp2-69. *Gene Expr.* 2003;11:163–179.
- Stevenson LF, Sparks A, Allende-Vega N, Xirodimas DP, Lane DP, Saville MK. The deubiquitinating enzyme USP2a regulates the p53 pathway by targeting Mdm2. *EMBO J.* 2007;26:976–986. doi: 10.1038/sj.emboj.7601567.
- Hong C, Duij S, Jalonen P, Out R, Scheer L, Sorrentino V, Boyadjian R, Rodenburg KW, Foley E, Korhonen L, Lindholm D, Nimpf J, van Berkel TJ, Tontonoz P, Zelcer N. The E3 ubiquitin ligase IDOL induces the degradation of the low density lipoprotein receptor family members VLDLR and ApoER2. *J Biol Chem.* 2010;285:19720–19726. doi: 10.1074/jbc.M110.123729.

30. Scotti E, Hong C, Yoshinaga Y, Tu Y, Hu Y, Zelcer N, Boyadjian R, de Jong PJ, Young SG, Fong LG, Tontonoz P. Targeted disruption of the idol gene alters cellular regulation of the low-density lipoprotein receptor by sterols and liver x receptor agonists. *Mol Cell Biol*. 2011;31:1885–1893. doi: 10.1128/MCB.01469-10.
31. Seidah NG. PCSK9 as a therapeutic target of dyslipidemia. *Expert Opin Ther Targets*. 2009;13:19–28. doi: 10.1517/14728220802600715.
32. Allende-Vega N, Sparks A, Lane DP, Saville MK. MdmX is a substrate for the deubiquitinating enzyme USP2a. *Oncogene*. 2010;29:432–441. doi: 10.1038/onc.2009.330.
33. Haimerl F, Erhardt A, Sass G, Tiegs G. Down-regulation of the de-ubiquitinating enzyme ubiquitin-specific protease 2 contributes to tumor necrosis factor- $\alpha$ -induced hepatocyte survival. *J Biol Chem*. 2009;284:495–504. doi: 10.1074/jbc.M803533200.
34. Liu Z, Zanata SM, Kim J, Peterson MA, Di Vizio D, Chirieac LR, Pyne S, Agostini M, Freeman MR, Loda M. The ubiquitin-specific protease USP2a prevents endocytosis-mediated EGFR degradation. *Oncogene*. 2013;32:1660–1669. doi: 10.1038/onc.2012.188.
35. Komander D, Reyes-Turcu F, Licchesi JD, Odenwaelder P, Wilkinson KD, Barford D. Molecular discrimination of structurally equivalent Lys 63-linked and linear polyubiquitin chains. *EMBO Rep*. 2009;10:466–473. doi: 10.1038/embor.2009.55.
36. Virdee S, Ye Y, Nguyen DP, Komander D, Chin JW. Engineered diubiquitin synthesis reveals Lys29-isopeptide specificity of an OTU deubiquitinase. *Nat Chem Biol*. 2010;6:750–757. doi: 10.1038/nchembio.426.
37. Zaaroor-Regev D, de Bie P, Scheffner M, Noy T, Shemer R, Heled M, Stein I, Pikarsky E, Ciechanover A. Regulation of the polycomb protein Ring1B by self-ubiquitination or by E6-AP may have implications to the pathogenesis of Angelman syndrome. *Proc Natl Acad Sci U S A*. 2010;107:6788–6793. doi: 10.1073/pnas.1003108107.
38. Herman-Bachinsky Y, Ryoo HD, Ciechanover A, Gonen H. Regulation of the Drosophila ubiquitin ligase DIAP1 is mediated via several distinct ubiquitin system pathways. *Cell Death Differ*. 2007;14:861–871. doi: 10.1038/sj.cdd.4402079.
39. Silke J, Kratina T, Chu D, Ekert PG, Day CL, Pakusch M, Huang DC, Vaux DL. Determination of cell survival by RING-mediated regulation of inhibitor of apoptosis (IAP) protein abundance. *Proc Natl Acad Sci U S A*. 2005;102:16182–16187. doi: 10.1073/pnas.0502828102.
40. Weissman AM, Shabek N, Ciechanover A. The predator becomes the prey: regulating the ubiquitin system by ubiquitylation and degradation. *Nat Rev Mol Cell Biol*. 2011;12:605–620. doi: 10.1038/nrm3173.
41. Graner E, Tang D, Rossi S, Baron A, Migita T, Weinstein LJ, Lechpammer M, Huesken D, Zimmermann J, Signoretti S, Loda M. The isopeptidase USP2a regulates the stability of fatty acid synthase in prostate cancer. *Cancer Cell*. 2004;5:253–261.
42. Calvisi DF, Wang C, Ho C, Ladu S, Lee SA, Mattu S, Destefanis G, Delogo S, Zimmermann A, Ericsson J, Brozzetti S, Staniscia T, Chen X, Dombrowski F, Evert M. Increased lipogenesis, induced by AKT-mTORC1-RPS6 signaling, promotes development of human hepatocellular carcinoma. *Gastroenterology*. 2011;140:1071–1083. doi: 10.1053/j.gastro.2010.12.006.
43. Molusky MM, Li S, Ma D, Yu L, Lin JD. Ubiquitin-specific protease 2 regulates hepatic gluconeogenesis and diurnal glucose metabolism through 11 $\beta$ -hydroxysteroid dehydrogenase 1. *Diabetes*. 2012;61:1025–1035. doi: 10.2337/db11-0970.

## Novelty and Significance

### What Is Known?

- The E3-ubiquitin ligase inducible degrader of the low-density lipoprotein (LDL) receptor (IDOL) promotes ubiquitylation and subsequent degradation of the low-density lipoprotein receptor (LDLR), and thereby modulates LDL metabolism.
- Common and rare genetic variation in *IDOL* associates with the circulating level of LDL-cholesterol in humans.

### What New Information Does This Article Contribute?

- The deubiquitylase ubiquitin-specific protease 2 (USP2) interacts with IDOL.
- USP2 deubiquitylates IDOL leading to its stabilization, which paradoxically attenuates degradation of the LDLR by IDOL.
- USP2, IDOL, and the LDLR form a tri-partite complex in which USP2 can deubiquitylate the LDLR and prevent its degradation.

The E3 ubiquitin ligase IDOL promotes ubiquitylation and subsequent degradation of the LDLR. As such, IDOL activity represents an acute mechanism to shut down uptake of LDL-derived cholesterol into cells. Yet IDOL also promotes its own ubiquitylation and degradation and is, therefore, a highly unstable protein. Using a genetic approach, we identified the deubiquitylase USP2 as an IDOL-interacting partner. We found that USP2 deubiquitylates IDOL resulting in increased IDOL stability. However, despite elevated levels of IDOL degradation of the LDLR is paradoxically attenuated. Conversely, silencing of *USP2* expression enhances IDOL-dependent degradation of the LDLR. Underlying these observations, we demonstrate that IDOL, USP2, and the LDLR can form a tri-partite complex in which USP2 can deubiquitylate the LDLR. As such, our study identifies USP2 as a new regulator of LDL metabolism owing to its ability to counteract IDOL-mediated degradation of the LDLR. Furthermore, this finding emphasizes the important role of the ubiquitin-proteasomal system in lipoprotein metabolism and cardiovascular disease.

## The Deubiquitylase USP2 Regulates the LDLR Pathway by Counteracting the E3-Ubiquitin Ligase IDOL

Jessica Kristine Nelson, Vincenzo Sorrentino, Rossella Avagliano Trezza, Claire Heride, Sylvie Urbe, Ben Distel and Noam Zelcer

*Circ Res.* 2016;118:410-419; originally published online December 14, 2015;

doi: 10.1161/CIRCRESAHA.115.307298

*Circulation Research* is published by the American Heart Association, 7272 Greenville Avenue, Dallas, TX 75231

Copyright © 2015 American Heart Association, Inc. All rights reserved.

Print ISSN: 0009-7330. Online ISSN: 1524-4571

The online version of this article, along with updated information and services, is located on the World Wide Web at:

<http://circres.ahajournals.org/content/118/3/410>

Data Supplement (unedited) at:

<http://circres.ahajournals.org/content/suppl/2015/12/14/CIRCRESAHA.115.307298.DC1.html>

**Permissions:** Requests for permissions to reproduce figures, tables, or portions of articles originally published in *Circulation Research* can be obtained via RightsLink, a service of the Copyright Clearance Center, not the Editorial Office. Once the online version of the published article for which permission is being requested is located, click Request Permissions in the middle column of the Web page under Services. Further information about this process is available in the [Permissions and Rights Question and Answer](#) document.

**Reprints:** Information about reprints can be found online at:  
<http://www.lww.com/reprints>

**Subscriptions:** Information about subscribing to *Circulation Research* is online at:  
<http://circres.ahajournals.org/subscriptions/>

# **The deubiquitylase USP2 regulates the LDLR pathway by counteracting the E3-ubiquitin ligase IDOL**

Jessica Kristine Nelson, MSc<sup>1,3</sup>, Vincenzo Sorrentino, PhD<sup>1,3</sup>, Rossella Avagliano Trezza, MSc<sup>1</sup>, Claire Heride, PhD<sup>2</sup>, Sylvie Urbe, PhD<sup>2</sup>, Ben Distel, PhD<sup>1</sup>, and Noam Zelcer, PhD<sup>1,4</sup>

<sup>1</sup> Department of Medical Biochemistry, Academic Medical Center of the University of Amsterdam, Amsterdam, 1105AZ, The Netherlands, <sup>2</sup> Department of Cellular and Molecular Physiology, University of Liverpool, Liverpool, L69 3BX, United Kingdom

## **SUPPLEMENTAL MATERIAL**

## **Materials and methods**

### **Reagents**

Simvastatin and the proteasome inhibitor MG-132 were from Calbiochem. Lipoprotein deficient serum (LPDS) was prepared following standard procedures and confirmed to contain no lipoproteins (not shown). GW3965, and Bafilomycin A1 were from Sigma.

### **Cell culture and transfections**

HEK293T, HeLa, Huh7, and HepG2 cells were obtained from the ATCC. Cells were maintained in DMEM supplemented with 10% FBS at 37 °C and 5% CO<sub>2</sub>. A431 cells were a kind gift from Drs. Vilja Pietiainen and Elina Ikonen (University of Helsinki). Wildtype and *Idol*<sup>(-/-)</sup> MEFs were a kind gift from Dr. Peter Tontonoz (University of California at Los Angeles). DU145 were from Dr. Koen van de Wetering (NKI, Amsterdam). Where indicated, cells were sterol-depleted by culture in sterol-depletion medium (DMEM supplemented by 10% LPDS, 5 µg/mL simvastatin, and 100 µM mevalonate) or treated with 1 µM GW3965 to induce LXR signaling. HEK293T and HepG2 cells were transfected with the indicated amounts of plasmids using the JetPrime reagent. In transfection experiments the efficiency of transfection was monitored by co-transfection of an expression plasmid for GFP and was consistently >85% in HEK293T and HepG2 cells.

### **Plasmids and expression constructs**

Expression plasmids encoding IDOL, IDOL-FERM, LDLR, USP8, VLDLR, GFP, Ubiquitin, and Epsin1 were previously reported<sup>1-3</sup>. Expression plasmids encoding *USP2-69* and *USP2-45* cDNAs were generated with gateway-mediated recombination (Invitrogen). In experiments where only expression constructs for USP2-69 are used, USP2-69 is indicated just as USP2. The activity disabling C276A<sup>4,5</sup> mutation in USP2 was introduced using the QuikChange site-directed mutagenesis kit. All plasmids used in this study experiments were isolated by CsCl<sub>2</sub> gradient centrifugation and their correctness verified by sequencing.

### **Antibodies and immunoblot Analysis**

Total cell lysates were prepared in RIPA buffer (150 mM NaCl, 1% Nonidet P-40, 0.1% sodium deoxycholate, 0.1% SDS, 100 mM Tris-HCl, pH 7.4) supplemented with protease inhibitors. Lysates were cleared by centrifugation at 4 °C for 10 min at 10,000 g. Protein concentration was determined using the Bradford assay with BSA as reference. Samples (10–40µg) were separated on NuPAGE BisTris gels and transferred to nitrocellulose. Membranes were probed with the following antibodies: LDLR (Epitomics, clone EP1553Y 1:4000), tubulin (Sigma, clone DM1A, 1:5000), FLAG-HRP (Sigma, clone M2, 1:1000), GFP (affinity purified rabbit polyclonal anti-GFP was from Dr. Mireille Riedinger, UCLA, 1:5000, or Santa Cruz, clone B-2, 1:3000), MYC (Cell Signaling, clone 9B11, 1:4000), HA (Covance, clone 16B12, 1:10000), Ubiquitin (ENZO, clone FK2, 1:1000), Epsin1 (rabbit polyclonal serum raised against amino acids 249–401 of rat Epsin1, 1:5), His<sub>6</sub> (Rockland, 1:1000), EGFR (affinity purified rabbit polyclonal anti-EGFR sera was from Dr. Simona Polo, 1:40,000). Secondary HRP-conjugated antibodies (Zymed Laboratories Inc.) were used and visualized with chemiluminescence on a Fuji LAS4000 (GE Healthcare). All immunoblots are representative of at least three independent experiments.

### **LDL uptake assay**

DyLight 488-labeled LDL was produced as previously described<sup>6</sup>. Briefly, HepG2, HeLa, or A431 cells were incubated in sterol-depletion medium for 16 h prior to addition of LDL to increase LDLR abundance. To initiate LDL uptake, cells were washed twice with PBS and

incubated with 5  $\mu\text{g}/\text{mL}$  DyLight488-labeled LDL in DMEM supplemented with 0.5% BSA for the indicated time at 37°C. Subsequently, cells were washed twice with PBS supplemented with excess sterols (PBS with 10% FCS), followed by an additional wash with PBS. Endocytosis of LDL was measured by lysing cells in RIPA buffer and quantification of the fluorescence signal on a Typhoon imager. Relative LDL uptake was calculated from the measure of fluorescence values corrected for specific uptake (cells treated with labeled LDL in the presence of an excess of non-labeled LDL) and presented as mean  $\pm$  SD.

### Measurement of cell-surface LDLR

Cells were treated as indicated, dissociated with TrypLE Express and incubated in FACS blocking buffer (FACS buffer containing 2% goat serum) for 30 min on ice. Subsequently, 100,000 cells were stained in 50 $\mu\text{L}$  FACS buffer with a R-Phycoerythrin (PE)-conjugated mouse anti-human LDLR antibody (R&D Systems, #FAB2148P, 1:40) for 1 h on ice. Cells were subsequently washed three times with FACS buffer and directly analyzed on a FACSCalibur Flow Cytometer (BD Biosciences). Viable cells were gated and 10,000 events per condition acquired. Data were analyzed using the CellQuest software package. Relative surface LDLR was calculated from geomean values corrected for background (non-stained cells), and presented as mean  $\pm$  SD.

### siRNA transfection

To knockdown USP2 expression we used the ON-TARGETplus Human USP2 SMARTpool (Dharmacon: cat#L-006069-00), or the individual ON-TARGETplus Human USP2 siRNAs (Dharmacon: cat#J-006069-11, J-006069-12, J-006069-13). As control we used the ON-TARGETplus Non-targeting Pool (Dharmacon: cat#D001810-10). A431 and HeLa cells were transfected with control or USP2 siRNAs (final concentration 30 nM) using the JetPrime reagent. HepG2 and DU145 cells were transfected similarly, but with the RNAiMAX reagent. The efficiency of USP2 silencing was assessed by quantitative PCR. Unless otherwise indicated, siRNA transfection experiments were conducted for 48 hours.

### RNA isolation and quantitative PCR

Total RNA was isolated from cells using TRIzol and one microgram of total RNA was reverse-transcribed using the iScript reverse transcription reagent. SYBR Green real-time quantitative PCR assays were performed on a Lightcycler 480 II apparatus. Oligonucleotide sequences are available upon request.

### Yeast two-hybrid screen

*S. cerevisiae* strains used in this study are PJ69-4a (*trp1-901 leu2-3,112 ura3-52 his3-200 gal4D gal80D LYS2::GAL1-HIS3 GAL2-ADE2 met2::GAL7-lacZ*) and PJ69-4 $\alpha$  (*trp1-901 leu2-3,112 ura3-52 his3-200 gal4D gal80D LYS2::GAL1-HIS3 GAL2-ADE2 met2::GAL7-lacZ*). Cells were grown at 28 °C in YPAD (2% glucose, 2% peptone, 1% yeast extract and 4 mg/ml adenine) or in minimal glucose medium containing 0.67% Yeast Nitrogen Base (YNB) without amino acids, 2% glucose and amino acids as needed (2 mg/ml uracil, 3 mg/ml leucine, 2 mg/ml tryptophane, 2 mg/ml histidine, 4 mg/ml adenine, 2 mg/ml methionine). The yeast-two-hybrid screening was performed as following. PJ69-4 $\alpha$  transformed with human IDOL constructs or LDLR intracellular tail (residues 780-860) cloned into pACT2-DEST, and PJ69-4a transformed with the bait constructs cloned into pGDBU-DEST were selected on minimal agar plates lacking leucine or uracil, respectively. For mating, cells were pre-cultured for 16h in selection medium, and subsequently  $2 \times 10^6$  of transformed PJ69-4a and PJ69-4 $\alpha$  cells (1:1 ratio) were mated in 2xYPAD (4% glucose, 4% peptone, 2% yeast extract and 8 mg/ml adenine) for 24 hrs with slow shaking (50 rpm). Diploids were selected on minimal glucose plates lacking both leucine and uracil. To reconfirm interactions we used a spot assay. Briefly, diploid cells were incubated for 16 hrs in minimal glucose medium lacking leucine and uracil, diluted to OD<sub>600</sub> of 0.2 and grown till an OD<sub>600</sub> of 1. Cells were

then washed with sterile water and serially diluted so as to plate  $10^2$ - $10^5$  cells/spot on minimal glucose agar lacking leucine and uracil, and with or without histidine, 10-20 mM 3-aminotriazol (3-AT), and adenine. Plates were incubated for 3 days before analysis.

### ***Statistical Analysis***

Data are presented as mean  $\pm$  SD. One-way ANOVA followed by the Bonferroni correction was performed for comparison of more than two groups. Student's t-test was performed for comparison of two groups. P values of  $<0.05$  were considered significant.

### ***References***

1. Zelcer N, Hong C, Boyadjian R, Tontonoz P. LXR regulates cholesterol uptake through Idol-dependent ubiquitination of the LDL receptor. *Science*. 2009;325:100–104.
2. Sorrentino V, Nelson JK, Maspero E, Marques ARA, Scheer L, Polo S, Zelcer N. The LXR-IDOL axis defines a clathrin-, caveolae-, and dynamin-independent endocytic route for LDLR internalization and lysosomal degradation. *J Lipid Res*. 2013;54:2174–2184.
3. Sorrentino V, Scheer L, Santos A, Reits E, Bleijlevens B, Zelcer N. Distinct functional domains contribute to degradation of the low density lipoprotein receptor (LDLR) by the E3 ubiquitin ligase inducible Degradation of the LDLR (IDOL). *J Biol Chem*. 2011;286:30190–30199.
4. Shan J, Zhao W, Gu W. Suppression of cancer cell growth by promoting cyclin D1 degradation. *Molecular Cell*. 2009;36:469–476.
5. Oh KH, Yang SW, Park JM, Seol JH, Iemura S, Natsume T, Murata S, Tanaka K, Jeon YJ, Chung CH. Control of AIF-mediated cell death by antagonistic functions of CHIP ubiquitin E3 ligase and USP2 deubiquitinating enzyme. *Cell Death Differ*. 2011;18:1326–1336.
6. Motazacker MM, Pirruccello J, Huijgen R, *et al*. Advances in genetics show the need for extending screening strategies for autosomal dominant hypercholesterolaemia. *Eur Heart J*. 2012;33:1360–1366.

## Online figure legends

**Online figure I. Summary of IDOL-DUB yeast-two-hybrid screen.** Y2H assay for (A) USP2-LDLR<sub>IC</sub> and (B) IDOL-USP2. The corresponding IDOL constructs that were used are illustrated in [Fig. 1A](#). The intracellular tail of the LDLR or the different IDOL fragments and USP2 were cloned into yeast-two-hybrid “prey” and “bait” plasmids, respectively, and transformed into yeast. Haploid cells were mated, and diploid cells were serially diluted and plated on selective plates. The assay was performed as described in the Methods section, and decreasing amounts of cells are spotted and selected as indicated.

**Online figure II. The DUB USP2 is a novel binding partner of IDOL.** (A,B) HEK293T cells were transfected with 1:1 ratio of the indicated constructs for IDOL and the USP2 wildtype or catalytic mutant. Total cell lysates were immunoblotted or immunoprecipitated and analyzed as indicated. (C) Schematic representation of UPS2 functional domains. USP2, also known as USP2-69, has a N-terminal extension, involved in contacts with other proteins, and a C-terminal catalytic domain. Mutation of the key cysteine C276 residue in this domain impairs USP2’s DUB activity. USP2-45 is a shorter isoform of USP2, with a partial truncation of its N-terminal domain, but intact catalytic domain. This isoform also interacts with IDOL, as shown in [Fig. 1D](#).

**Online figure III. USP2 deubiquitylates and stabilizes IDOL.** HEK293T cells were transfected with the indicated IDOL and USP2 expression vectors, with a ratio of IDOL:USP2 of 1:5 (left panel) or 1:10 (right panel). 48 hours after transfection, cells were incubated for the indicated times with 10 µg/mL cycloheximide (CHX), and cells harvested for immunoblots and kinetic analysis as shown in [Fig. 2C](#).

**Online figure IV. Silencing USP2 reduces the level of ectopic IDOL protein.** (A) HepG2 and (B) Huh7 cells were co-transfected with IDOL and GFP expression plasmids, and either Control (Non-targeting, NT) or *USP2* siRNA. 48 hours later total cell lysates were collected and immunoblotted as indicated. A representative immunoblot of three independent experiments is shown. (A,B) the intensity of IDOL protein was quantified and normalized to that of GFP. The relative IDOL protein level is plotted. Each bar and error represent the mean ± SD (N=3). \*  $p < 0.05$

**Online figure V. USP2 attenuates IDOL and LXR-induced degradation of the LDLR.** (A) HEK293T cells were transfected with LDLR and with IDOL and USP2-45 (1:7 ratio). 48 hours after transfection, cells were collected and immunoblotted as indicated. (B,C) HeLa cells were transfected with the indicated USP2 expression vector. 48 hours after transfection, cells were treated with 1 µM GW3965 (GW) for 4 hours to activate the LXR pathway and subsequently harvested for (B) immunoblots and (C) qPCR analysis as shown (n=4, \*\*\*  $p < 0.001$ ). Expression of USP2 does not affect LXR activation, as shown by the increased expression of *IDOL* and *ABCA1*. (D) HepG2 cells were cultured in complete medium or in sterol-depletion medium for 16 hours, and subsequently treated with vehicle or 1 µM GW3965 (GW) for 4 hours. The mRNA levels of *USP2*, *LDLR* and *IDOL* were analyzed as indicated. Expression of *USP2* is not affected by LXR activation or by variations in the cellular sterol content (n=5, \*\*\*  $p < 0.0001$ ).

**Online figure VI. USP2 silencing decreases LDLR protein levels in different cell lines.** (A) Relative IDOL expression in the indicated cell lines was determined by qPCR. Each bar and error represent the mean ± SD of three independent experiments (B) HeLa and DU145 cells were transfected as indicated with 30 nM of control (Non-targeting, NT) or *USP2* siRNA. 48 hours after transfection cells were shifted to sterol-depletion medium for an additional 24 hours after which total cell lysates were collected and analyzed by immunoblotting. (C,D) A431 and DU145 cells were cultured and treated as in (B) and

analyzed by qPCR to assess *LDLR*, *IDOL* and *USP2* mRNA levels (n=4, \* $p < 0.05$ ). (E) Wild-type and *Idol*<sup>(-/-)</sup> MEFs were cultured and treated as in **Fig. 4E**. 72 hours after transfection, cells were collected and analyzed by qPCR as indicated (n=4, \*\*\*  $p < 0.0001$ ). All immunoblots are representative of at least three independent experiments.

**Online figure VII. *USP2* silencing decreases LDLR protein levels (A,B)** The specificity of *USP2* silencing in HepG2 cells was tested by transfecting cells as indicated with 30 nM of a control (Non-targeting, NT), three individual *USP2* siRNAs, or with a pooled set of *USP2* siRNAs. 48 hours after transfection cells were shifted to sterol depletion medium for an additional 24 hours after which cells were collected and total cell lysates were analyzed by immunoblotting (**B**) or by qPCR (**A**) to assess the efficiency of *USP2* mRNA silencing (n=3, \*\*\* $p < 0.001$ ).

**Online figure VIII. Graphical scheme for the IDOL-USP2 nexus in regulation of the LDLR.** (A) IDOL expression is induced by activation of the sterol-sensing nuclear receptors LXRs. This leads to enhanced ubiquitylation of the LDLR, which targets the receptor for lysosomal degradation. In parallel, auto-ubiquitylation of IDOL leads to its proteasomal degradation. (B) *USP2* is recruited together with IDOL to the intracellular tail of the LDLR. There, *USP2* can counteract IDOL-mediated ubiquitylation of the LDLR by removing these chains from the receptor.

**Online table I**

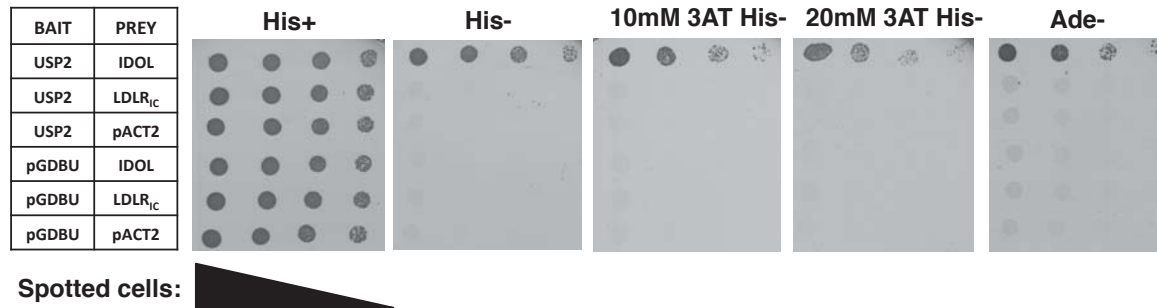
	BAIT			Diploids	
PREY	IDOL	IDOL Ring		IDOL	IDOL Ring
UCHL1			OTUB2		
USP11			EIF3S3		
USP28			USP19		
USP48B			USP38		
OTUD6A	*		CEZANNE		
ATXN3L			EIF3S5		
UCHL3			BAP1		
USP12			USP4		
USP30			USP20		
USP49			USP39		
OTUD5			VCPIP1		
JOSD1			PSMD7		
UCHL5			USP15		
USP13	*	*	USP5		
USP30			USP41B		
BRCC3			OTUD4		
JOSD2			PSMD14		
BAP1			AMSH	*	*
USP14			USP6		
USP32			USP44		
USP54			YOD1		
CSN5			USP7		
UBC13			USP25	*	
USP1			USP45		
USP33			TNFAIP3		
OTUB1			AMSH-LP		
CSN6			USP8		
FLJ14981			USP26		
<b>USP2-69</b>	<b>+++</b>		USP46		
USP16			OTUD6B		
USP36					

**Online table I: Identification of USP2 as a novel IDOL-binding partner by the Y2H assay**

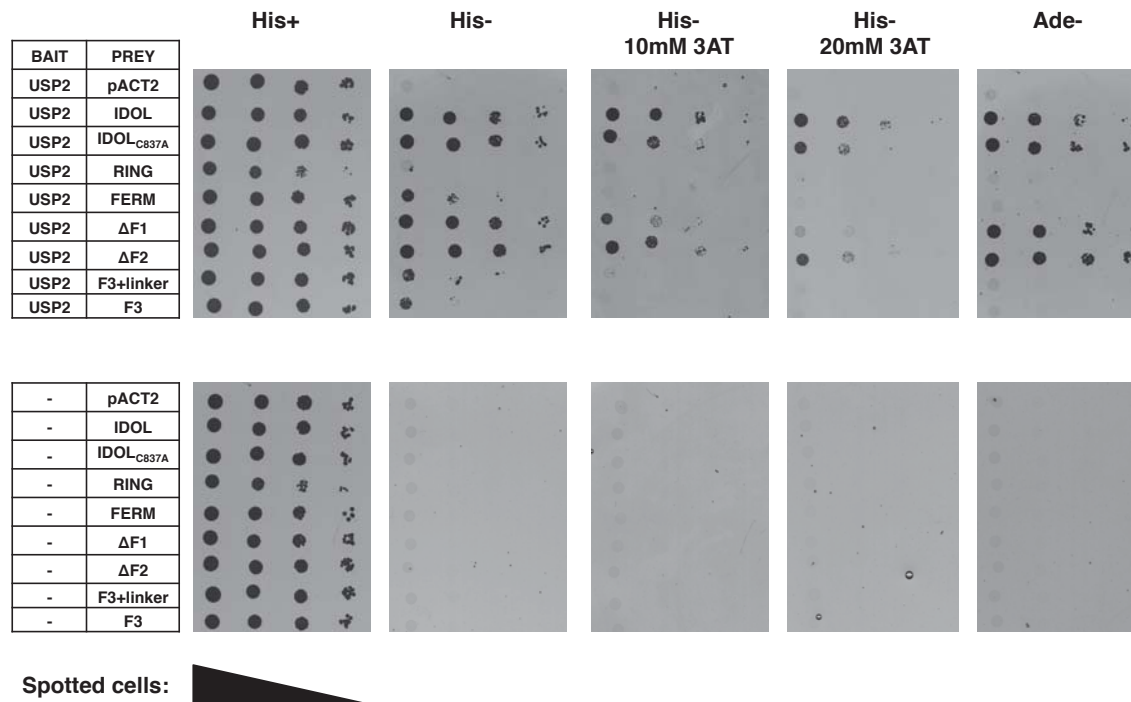
The full length IDOL, or its RING domain, was screened against a library of human DUBs, comprehensive of the listed enzymes. The assay was performed as described in the Methods section. False positives are indicated by the asterisk, and they represent DUBs whose co-expression in the yeast system with the empty pACT2-DEST vector resulted in selective cell growth even in the absence of IDOL or LDLR. Only yeast diploids co-expressing full length IDOL and USP2-69 showed marked growth on both selective media (+++), and were considered for validation analysis. A similar screen was performed using the LDLR intracellular tail, however it did not identify any potential LDLR-interacting DUBs.

# Online figure I

**A**

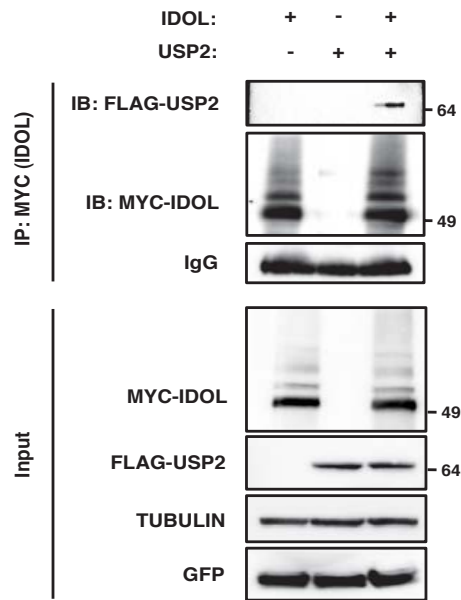


**B**

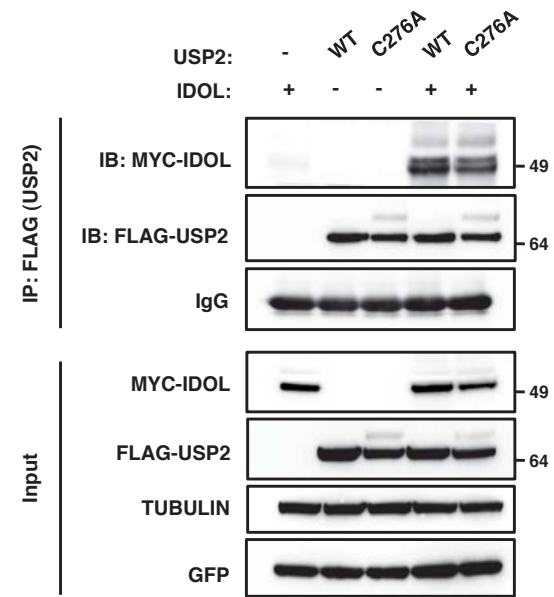


# Online figure II

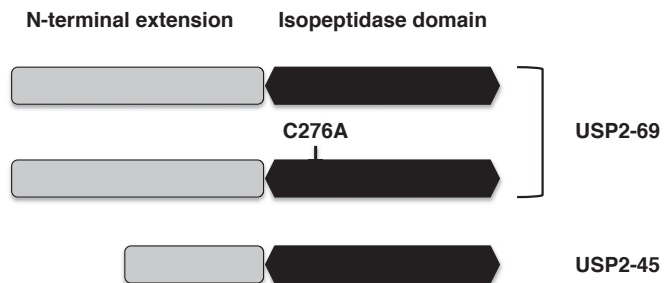
**A**



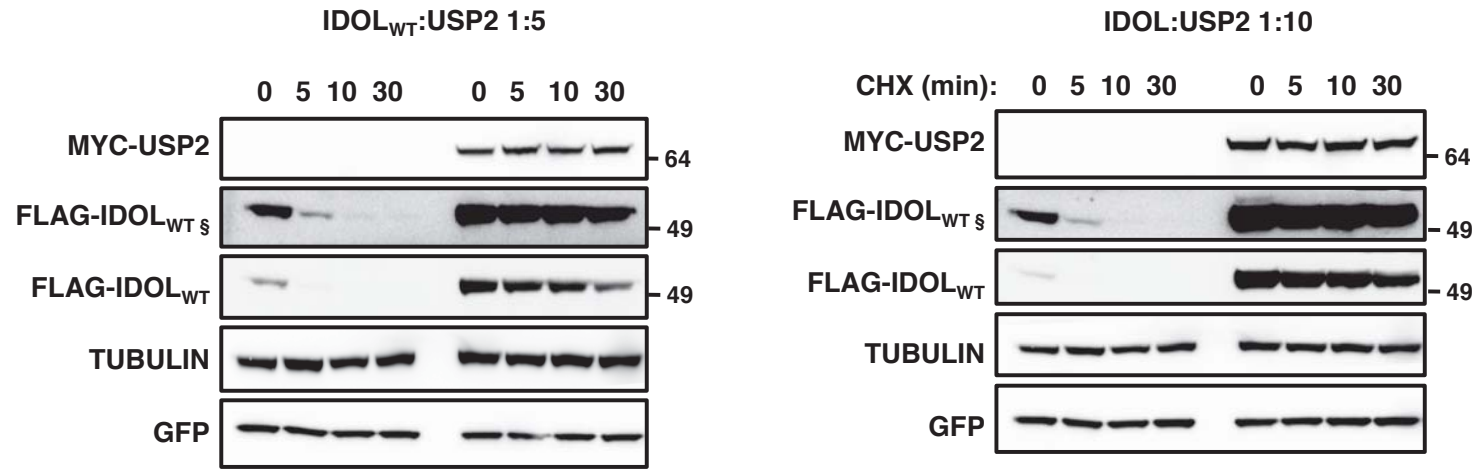
**B**



**C**

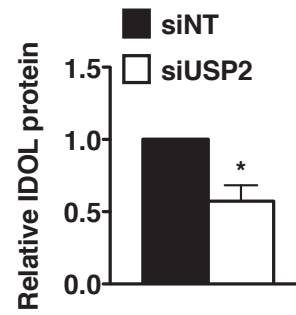
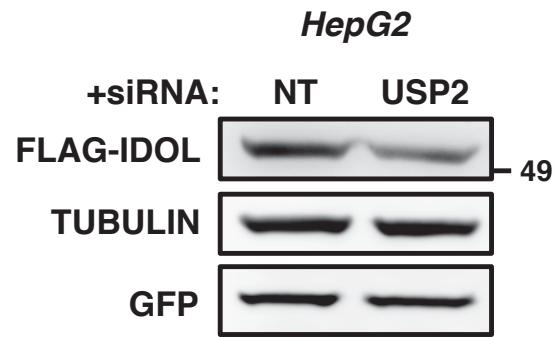


# Online figure III

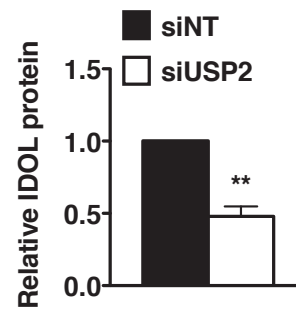
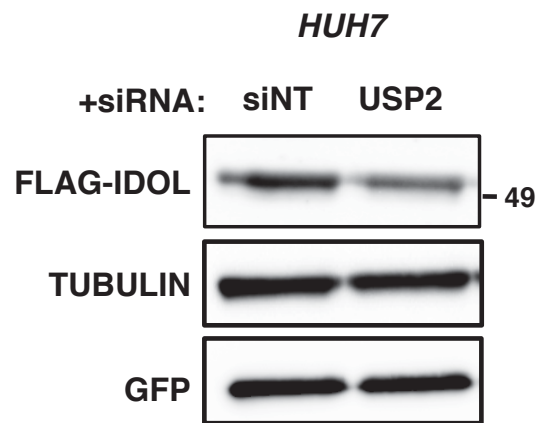


# Online figure IV

**A**

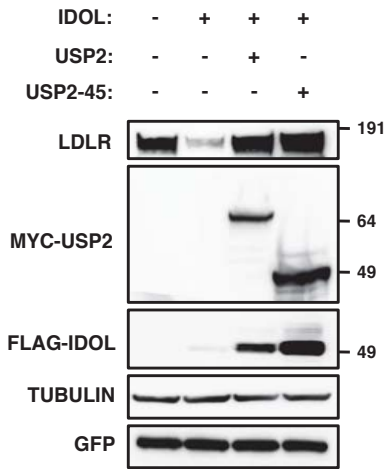


**B**

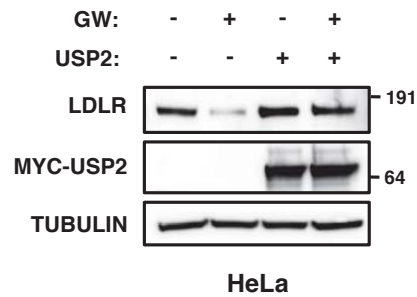


# Online figure V

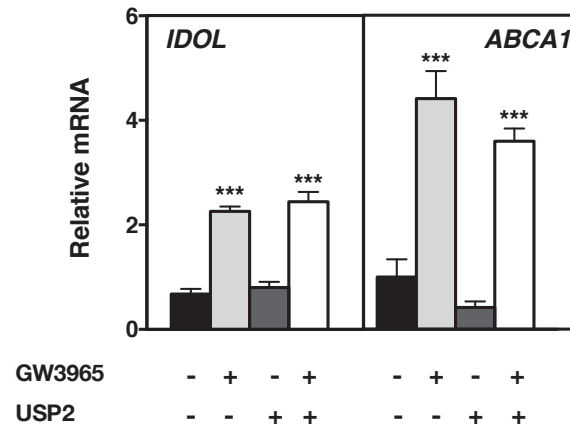
**A**



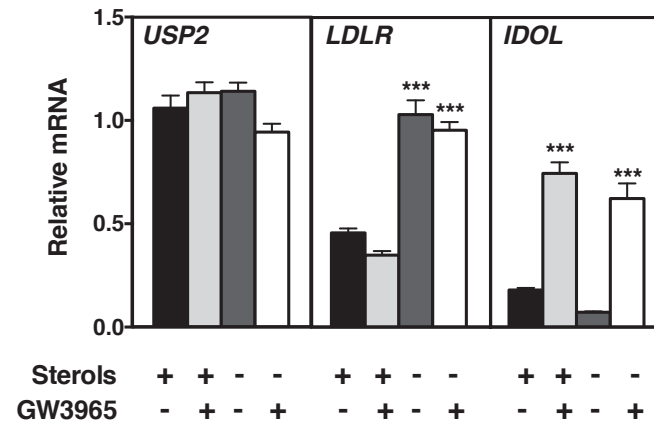
**B**



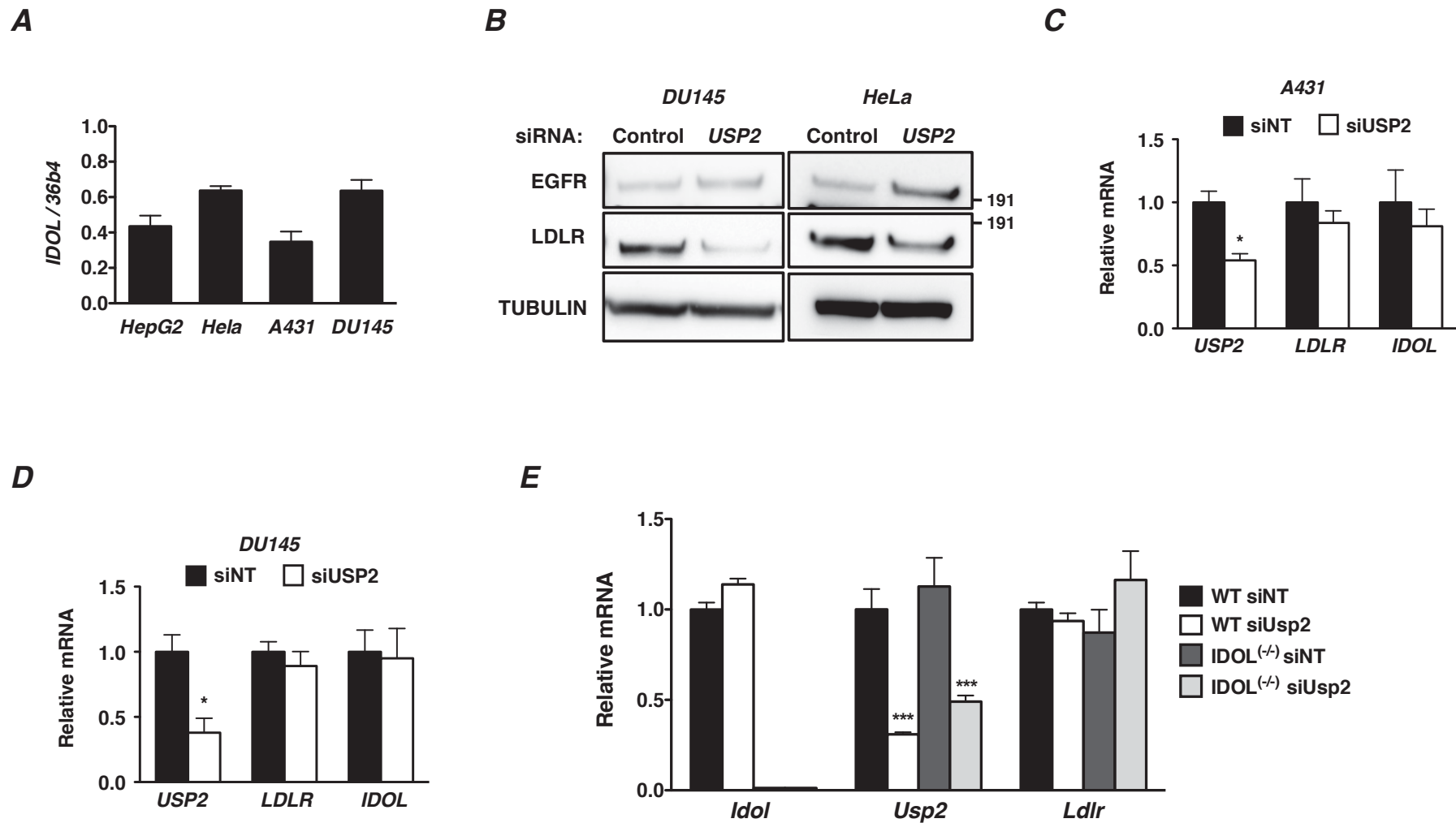
**C**



**D**

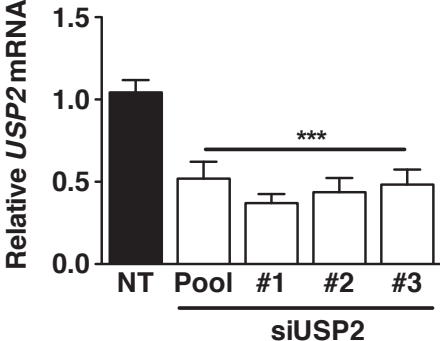


# Online figure VI

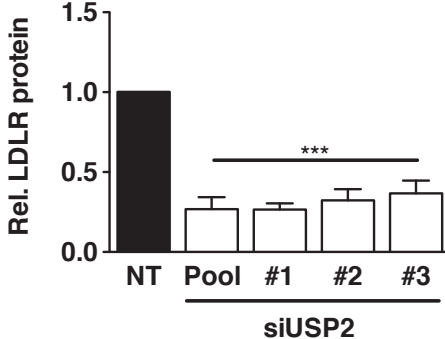
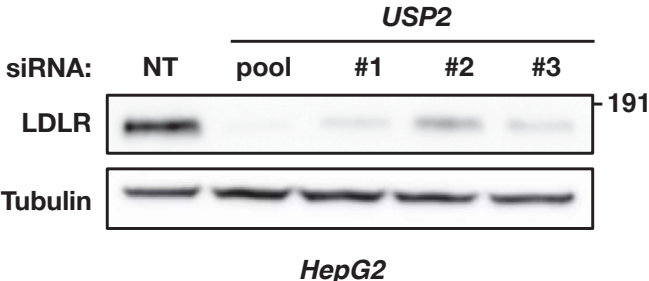


# Online figure VII

**A**



**B**



# Online figure VIII

